AD-A064 418 AIR FORCE INST OF TECH WRIGHT-PATTERSON AFB OHIO SCH--ETC F/G 20/12
ELECTRICAL CHARACTERIZATION OF GAAS ANODIC OXIDES USING ISOTHER--ETC(U)
DEC 78 M J BIANCALANA

UNCLASSIFIED AFIT/GE/EE/78-18 NL

END
DATE FILMED
4-79
DDC

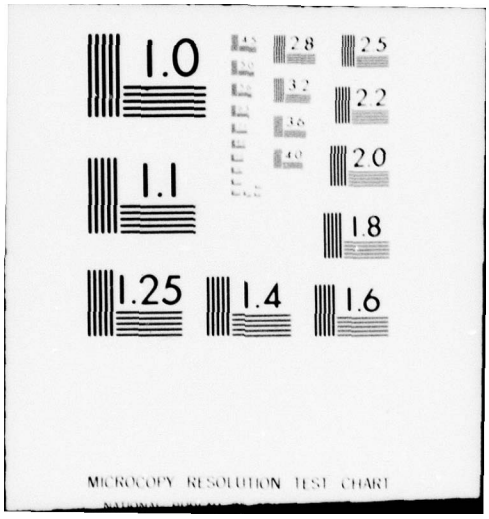
1.0
1.1
1.25
1.4
1.6
2.8
2.5
3.2
2.2
3.6
4.0
2.0
1.8
MICROCOPY RESOLUTION TEST CHART

DEC

D

AD A064418

DDC FILE COPY

LEVEL II

ELECTRICAL CHARACTERIZATION OF GaAs ANODIC OXIDES USING ISOTHERMAL DIELECTRIC RELAXATION CURRENT

THESIS

AFIT/GE/EE/78-18 Martin J. Biancalana
Capt USAF

DDC
RECEIVED
FEB 12 1979
A

80 01 30 143

(14) AFIT/GE/EE/78-18

(6) ELECTRICAL CHARACTERIZATION OF GaAs ANODIC OXIDES USING ISOTHERMAL DIELECTRIC RELAXATION CURRENT.

(9) Master's thesis,

THESIS

Presented to the Faculty of the School of Engineering

of the Air Force Institute of Technology

Air University

in Partial Fulfillment of the

Requirements for the Degree of

Master of Science

(16) 2305 (17) R1 (12) 79 p'

by

(10) Martin J. Biancalana

Capt USAF

Graduate Electrical Engineering

(11) December 1978

ACCESSION for
NTIS White Section
DDC Buff Section
UNANNOUNCED
JUSTIFICATION
BY
DISTRIBUTION/AVAILABILITY CODES
Dist. AVAIL. and/or SPECIAL
A

Approved for public release; distribution unlimited

012 225

Preface

This thesis involved the design, assembly, and use of a measuring system for dielectric films on GaAs. This particular system was decided upon after unsuccessful attempts to use capacitance-voltage and conduction techniques to characterize GaAs MOS sample devices. The bulk of the effort went into producing simple and reliable apparatus, operating under control of a programmable calculator. The software was designed to be easily modified, and the procedure involves no critical adjustments.

Thanks are due to Dr. Schuermeyer, Dr. Hartnagel, Dr. Bayraktaroglu, and Mr. Blasingame for their very helpful discussions. Dave Mays and his colleagues at the Avionics Laboratory provided a great deal of assistance in preparing the samples. Dr. Borky, Dr. Fontana, and Prof. Lubefeld deserve credit for reading and commenting on the manuscript that eventually became this thesis. Lastly, a special thanks to my wife, Jan, whose patience and encouragement greatly aided in the completion of this work.

M. J. Biancalana

Contents

List of Figures

List of Symbols

A	area of gate electrode
C_d	depletion layer capacitance
C_I	insulator capacitance
C_{ox}	oxide capacitance
d	thickness of the oxide
E_c	energy level of bottom of the conduction band
E_{Ft}	transient Fermi level
E_p	approximation to the transient Fermi level
E_v	energy level of top of the valence band
E_o	starting or initial energy
e_n	electron emmission probability
I	current
I_o	initial current
k	Boltzmann's constant
N_s	density of states
q	electronic charge
T	temperature
t	time
V_s	surface potential
ϵ_o	permitivity of free space
ϵ_r	relative dielectric constant
τ	time constant
ϑ	attempt to escape frequency

Abstract

The theory and practical limitations of the IDRC technique of Mar and Simmons are discussed. An improved version of the original experiment that incorporates digital processing of the data is described. Results were obtained for Si and used to establish confidence in the new procedure. Anodic oxides of GaAs were then studied, and the results indicate that there are large densities ($2 \times 10^{13} cm^{-3} eV^{-1}$) of both fixed and mobile trap states at and near the interface. The mobile trap states behave as though negatively charged. Limitations of the theory as applied to GaAs are discussed, and a complete software listing for the procedure is included.

ELECTRICAL CHARACTERIZATION OF GaAs ANODIC OXIDES USING ISOTHERMAL DIELECTRIC RELAXATION CURRENT

I. Introduction

Significance

This research is significant in that it adapts a measurement technique useful in Si MIS devices to the problem of measuring the electrical properties of GaAs passivation layers. The technique of isothermal dielectric relaxation current (IDRC) measurement is shown to provide useful results in GaAs measurements despite the complex nature of the GaAs MIS system. This work was done as part of the GaAs surface passivation effort being conducted by the Air Force Avionics Laboratory with the goal of developing devices for high speed logic and microwave systems to meet a variety of projected AF operational requirements.

Surface passivation is the process of forming an insulating, protective layer on a semiconductor substrate. An important property of this layer is its ability to neutralize the high density of carrier trap states normally present on a semiconductor surface. In Si technology the most common passivating layer is thermally grown or deposited SiO_2.

The passivation layer is the key to fabricating MOS or

MIS devices with any semiconductor. In these devices the passivating layer forms the gate insulation and accounts for the high input impedance characteristic of the device. Its properties also strongly influence threshold voltage, temperature stability, and other crucial device parameters.

Were MIS technology available for use with GaAs, the high electron mobility of this material would result in high speed devices. As discrete structures this would mean more efficient microwave devices than are possible in Si as well as achieving significant advantages over presently used Schottky barrier gate GaAs devices. In integrated form GaAs MIS circuits are expected to achieve gigabit speeds. Since GaAs can be made into lasers and detectors already, a capability to fabricate MIS circuits with this material could lead to complete high speed communications systems on a single substrate.

Background

Unfortunately, surface passivation of GaAs is a much more difficult problem than passivation of Si. The problem is that GaAs is unstable at the temperature needed to grow thermal oxides, and that As_2O_5 has a very high vapor pressure above 560°C. When As_2O_5 evaporates from native oxide Ga_2O_3 is left. This is a porous crystalline material that is unsuitable for passivation.

Layers of other materials such as Si_3N_4 have been sputtered or evaporated on GaAs to act as a passivating

layer. These are again too porous, and leave a very high density of surface trap states. Attempts to improve the surface state density problem by annealing are thwarted by the thermal instabilities of GaAs and As_2O_5, and the porosity of the layers.

Recently another technique, anodic oxidation, has been shown to be very promising. Work by H. Hartnagel (Ref 1) and others has shown that dense layers of native oxide can be formed at room temperatures.

This method involves placing the GaAs surface to be passivated as the anode in an electrolytic cell with an inert cathode. A current is started through the cell by either a current or voltage source. Whichever parameter, current or voltage, is controlled, the other is monitored to give an extremely accurate indication of the progress of the anodization. When sufficient oxide has been grown, the substrate is removed from the electrolyte. Since the common solvents used in the electrolysis bath are ethylene glycol and water or ammonium pentaborate for non-aqueous work, this is an inherently low temperature process. The resulting oxides may be annealed at temperatures as high as 350°C without deterioration.

In addition to native oxides, more complex layered structures have been formed. Aluminum sputtered onto the GaAs substrate before anodization forms a layer of Al_2O_3 during anodization. The aluminum oxide forms first since Al is more chemically active than either Ga or As. Once

the layer has been formed, it is possible with some electrolytes to form native oxide either over the Al_2O_3 layer or under it. Growing the Al_2O_3 has the advantage of producing a better dielectric and allowing a higher safe anneal temperature.

Anodic oxidation is a simple and repeatable process. During the process the reaction rate is controlled by the driving variable, either a voltage or current source. The progress of the reaction can be ascertained by monitoring the other variable, either current or voltage respectively. This allows real time detection of abnormalities such as contamination of the electrolyte. It also greatly aids in achieving repeatable results.

Problem

This thesis project addresses the problem of determining the best anodization procedure to use by evaluating film properties to demonstrate empirically which anodic oxide (or any other insulator for that matter) produces the best dielectric for device structures. This reduces, in large degree, to a problem of measuring the surface state density. In Si the test used to determine this is a capacitance-voltage measurement. Surface state density is found from these measurements using a theoretical model of the structure. Conductance measurements rely on a similar model. These techniques fail when the assumptions inherent in the model are no longer valid, such as when the surface state density is very high or the dielectric becomes

lossy (Ref 2:131). Both of these exceptions occur with GaAs.

Surface state measurement is complicated further by the lack of detailed knowledge of the surface chemistry of GaAs, especially under anodic conditions. Also, the state of the art of growing bulk GaAs is still not comparable to that of Si. The result is a high level of surface defects in the basic crystal lattice. This is serious in itself, but there is the additional possibility of adsorbtion of a doping impurity, such as carbon, onto the surface before or during anodization. Complicating any speculation about the condition of the surface is the fact that carbon adsorbed on the surface could be at a concentration an order of magnitude lower than the level which is detectable by Auger analysis and yet produce a surface layer doping of around 10^{16} states per cm^3 for a depth of a few atomic layers. Carbon impurities produce p-type GaAs, i.e. very effective trap states, in otherwise n-type GaAs. Many such conceivable hypotheses about the GaAs surface have not been tested. What is known is that the surface state density is extremely high in GaAs MIS structures and is hindering progress toward MIS devices. It would be of great value to have a measure of these states and their position in the band gap. Such a measure is the goal of this research.

Approach

The approach taken in this work was to adopt a measurement technique, based on rather basic concepts, which has

been shown to work on Si; assemble it in improved form; demonstrate that the apparatus works as expected by measuring a Si sample; and finally use the method to explore GaAs.

The method chosen was that of isothermal dielectric relaxation current measurement. This technique was proposed by Simmons and Wei (Ref 3), and results were published on MNOS devices by Mar and Simmons (Ref 2). The theory is based on fundamental characteristics of semiconductors. Therefore, there should in principle be little trouble in applying it to GaAs. The method also should work well when a high density of states is present (Ref 2).

This method was originally implemented by its developers with completely analog apparatus. In the present apparatus the data are handled digitally, producing a simple operation. The digital data processing also allows for straightforward quantization of error in terms of sample standard deviation. The result is a useful measurement tool that is simple to operate and understand.

II. Theory

Theoretical Considerations for Silicon

The theory proposed by Simmons and Wei (Ref 3) provides the basis for this measurement. It is an attractive theory in several respects. The physics involved is fairly simple, and the measurement results directly in a plot of density of states vs. energy.

The theory uses the definition of the Fermi level and a description of how the Fermi level moves in energy as the bias on the sample is changed to derive an expression for the discharge current as a function of time and density of surface states. In an unbiased Si MOS structure, the energy distance diagram is as shown in Fig. 2-1. The Fermi level is flat, and due to surface states (typically 10^{10} or 10^{11} states per cm^2), some depletion is evident. When the sample is placed into accumulation during the experiment, the diagram changes to look like Fig. 2-2. Here the Fermi level in the semiconductor is displaced from that in the metal and the bands are bent as a result of the excess electrons at the interface. The shaded area represents the surface states that are now filled. The assumption is that all states below the Fermi level are filled during accumulation and the rest are empty. When the bias is changed to produce surface depletion, the diagram tends toward that shown in Fig. 2-3. This change cannot happen instantly due to

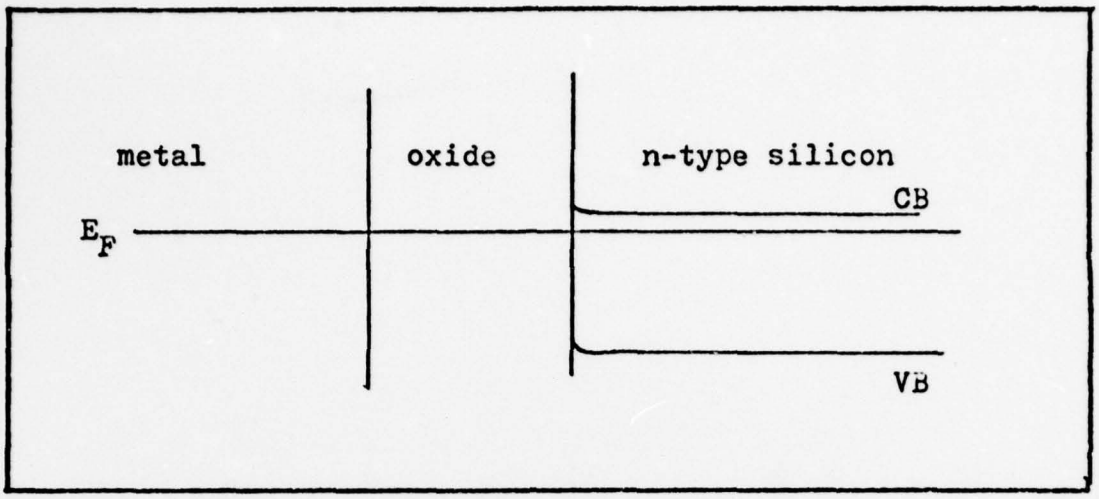

Fig. 2-1 Silicon MOS at zero bias.

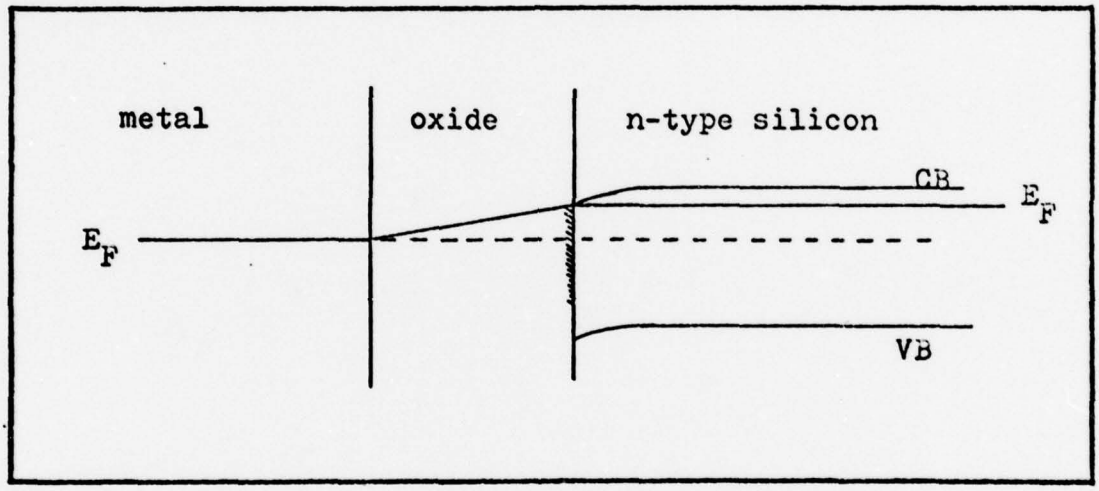

Fig. 2-2 Silicon MOS accumulated by external bias.

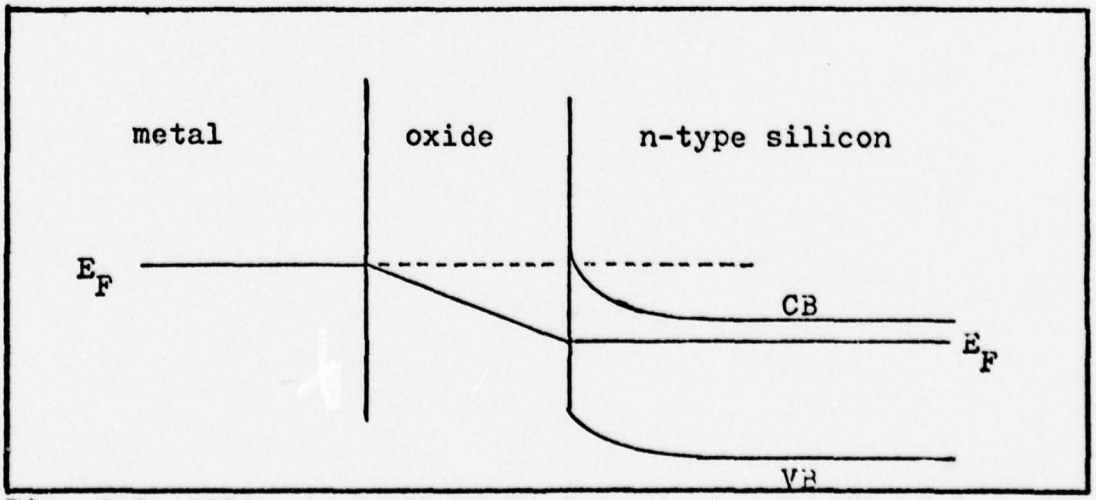

Fig. 2-3 Silicon MOS in depletion due to external bias.

the time constants of the states. Thus, during the transient the states in the top half of the band (n-type material is considered here) discharge in sequence moving the Fermi level toward the configuration in Fig. 2-3. This discharge forms a current in the external circuit that can be measured.

During the transient the Fermi level (E_{Ft}) is given by:

$$E_{Ft} = E_c - kT(\ln \vartheta t + .365) \qquad (1)$$

where

E_c = Energy at the bottom of the conduction band

k = Boltzmann's constant

T = temperature in ^oK

ϑ = attempt to escape frequency ($= v\sigma_n N_c$)

v = thermal velocity of electrons

σ_n = electron captive cross section for interface states

N_c = effective density of states in the C.B.

t = time in seconds.

This non-steady-state Fermi level is approximated by:

$$E_p = E_c - kT \ln \vartheta t \qquad (2)$$

where E_p is the approximated transient Fermi level.

From conservation of charge considerations the following expression for the current density due to the discharge is derived:

$$J = \frac{qC_I}{C_I+C_d}\int_{E_v}^{E_c} N_s(E)\ e_n\ \exp(-e_n t)dE \qquad (3)$$

where

q = electronic charge

C_I = insulator capacitance

C_d = depletion layer capacitance

E_v = energy at the top of the valence band

e_n = electron emission probability

$N_s(E)$ = surface state density as function of energy

By noticing that $e_n \exp(-e_n t)$ can be approximated by a delta function, the integral of Eq (3) can be closely approximated and solved in closed form. With the assumption that $C_I \gg C_d$ an expression for the current can be derived:

$$I(t) = \frac{qAkT}{t} N_s(E_p) \qquad (4)$$

where A is the area of the gate.

This equation can be rewritten as:

$$N_s(E_p) = \frac{I(t)\cdot t}{qAkT} \qquad (5)$$

to show that the density of states at the energy E_p is directly proportional to the current-time product.

With Eq (2) to transform the time axis, an $I(t)\cdot t$ vs. t plot can be rescaled to a plot of density of states vs. energy.

Practical Considerations

There are several aspects of the theory that did not explicitly appear in the original paper that definitely affect its use as a basis for laboratory measurements. The first of these is the fact that the range of any given isothermal measurement is limited. If at a given temperature the measurement could be taken from 10^{-5} second to 100 seconds the range in eV would be only .28 eV ($=10^{11}$Hz, T=200°K). This means that more than one isothermal measurement must be taken to explore the upper half of the band gap of silicon. However, there are more practical constraints to take into account.

If there are any states closer to the conduction band than the range of the measurement (.24 eV in this case), these states will discharge very quickly, and their discharge current can be approximated by that of a capacitor:

$$I(t) = I_o \exp(-t/\tau) \qquad (6)$$

where τ is the effective time constant of the measuring system.

When this is plotted as I·t vs. t there is always a maximum at $t=\tau$. Therefore, the actual measurement must not start until a time much greater than $t=\tau$. Again considering that the discharge can be approximated by Eq (6), after a long time the current will be too small to measure and all that will be in the system is noise. That noise will be

multiplied by an ever increasing t (time), so the noise will look like an increasing or wildly erratic density of states. These considerations lead to the establishment of a more practical measurement window of 10 seconds to 25 seconds.

To explore the states over the whole upper half of the band gap, it is necessary to vary the temperature. In doing this each measurement is isothermal, but at a different temperature. This makes temperature the variable that moves the measurement window to the place in the band gap to be explored. At liquid helium temperature the measurement can be as close as .01 eV from the conduction band. The other end of the measurement is always the midpoint of the band gap where holes produce a significant change in the current (in p-type material it would be electrons that upset the measurement).

As a result of these considerations, the apparatus was designed to measure the average isothermal dielectric relaxation current at any temperature, calculate the sample standard deviation of the averaged data sample, and form the I-t product. This is then plotted as a series of horizontal lines whose lengths represent the energy range of the measurement, and whose vertical positions represent the average density of states in that range. A vertical line through the midpoint of each horizontal line extends one standard deviation above and below each horizontal line.

Considerations for GaAs

There are known differences between GaAs MOS structures and their Si counterparts. It can be expected that some of these differences will affect the IDRC measurement.

The first significant difference is that it is not possible to bring native oxide MOS structures into accumulation (Ref 4). At a minimum, this has the effect of changing the scaling between time and energy, Eq (2). Since Eq (2) was derived from the occupation function which is part of the integral that defines the current density, Eq (3), it would seem that the current density function is also affected. This is not necessarily so. Since the integral in Eq (3) is evaluated by approximating the occupation function by a delta function, Eqs (4), (5) will be valid as long as this approximation is justified. However, while the density of trap states will remain proportional to $I \cdot t$, the energy scale will be in error. While the error will, at the least, produce a simple translation of the results in energy, it could also introduce expansion or contraction of the energy scale.

Another difference is that it is possible that the Fermi level is pinned. That is, the structure is not only prevented from reaching accumulation, but is also prevented from reaching deep depletion (Ref 5:2). Since a wide energy state structure has been observed using the IDRC technique, if this effect is present, it does not hamper the measurement.

The effects just considered are caused by the large density of trap states near the interface. The IDRC experiment is designed to investigate these states. In the present form of the apparatus, the IDRC data can be easily processed to yield information on the validity of the energy scale by calculating the change in surface potential represented by the discharge current observed and comparing that value to the actual change in bias. If the scale is valid, the bias change should be equal to or larger than the calculated change in surface potential.

The change in surface potential is calculated as a function of energy by:

$$V_s(E) = \frac{\int_{E_o}^{E} N_s \, dE}{C_{ox}} \tag{7}$$

$$C_{ox} = \frac{\epsilon_r \epsilon_o}{d} \tag{8}$$

where:

$V_s(E)$ = change in surface potential as a function of energy

E_o = initial energy

C_{ox} = oxide capacitance

ϵ_r = relative dielectric constant

ϵ_o = permittivity of free space

d = thickness of the oxide.

In calculating C_{ox}, ϵ_r was assumed to be 7.

III. Experiment

Equipment

The experiment is divided into three parts by function or operation. It is therefore convenient to describe it in terms of these parts: the analog section, the digital section, and the temperature controller. These sections are shown in Fig. 3-1.

The analog section consists of those instruments that directly interface with the sample. An HP 6200B power supply is used to produce bias voltages of plus and minus ten volts with respect to ground. A trigger unit, fabricated from standard parts, is used to adjust and switch the bias applied to the sample (Fig. 3-2). A Fluke 8100A digital volt meter (DVM) is used to monitor the bias voltage while it is being adjusted. This DVM is then removed from the circuit. The trigger unit switches bias voltages upon receipt of a trigger signal from the digital section. The leads of the sample header are soldered into the circuit with the gate lead connected to the output of the trigger unit and the substrate lead connected to the picoammeter. The picoammeter is a Keithly 417 High Speed Picoammeter, and is connected in series between the sample and ground. This meter has an output for a chart recorder which is used to interface with the digital section.

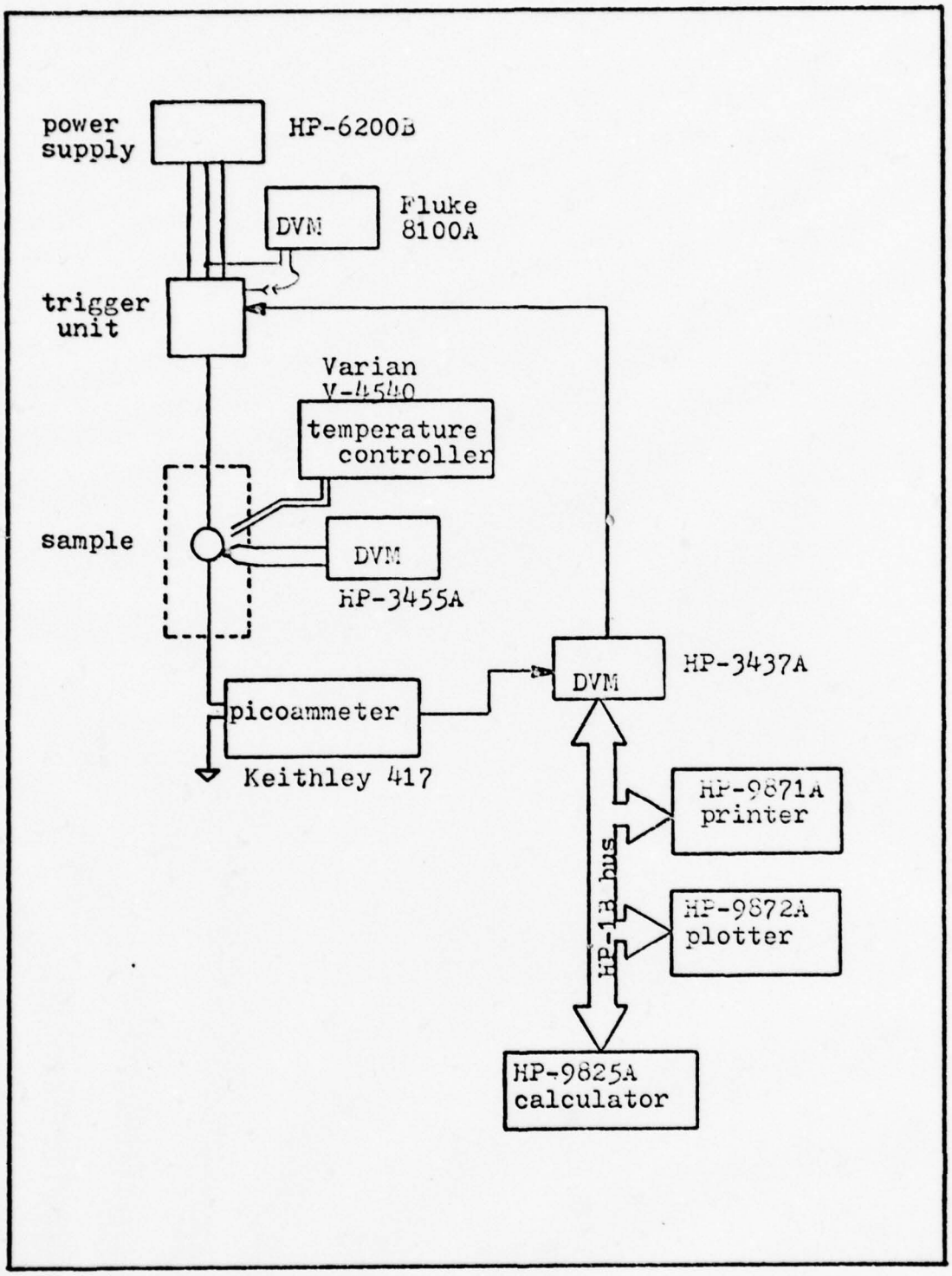

Fig. 3-1 Measurement system block diagram.

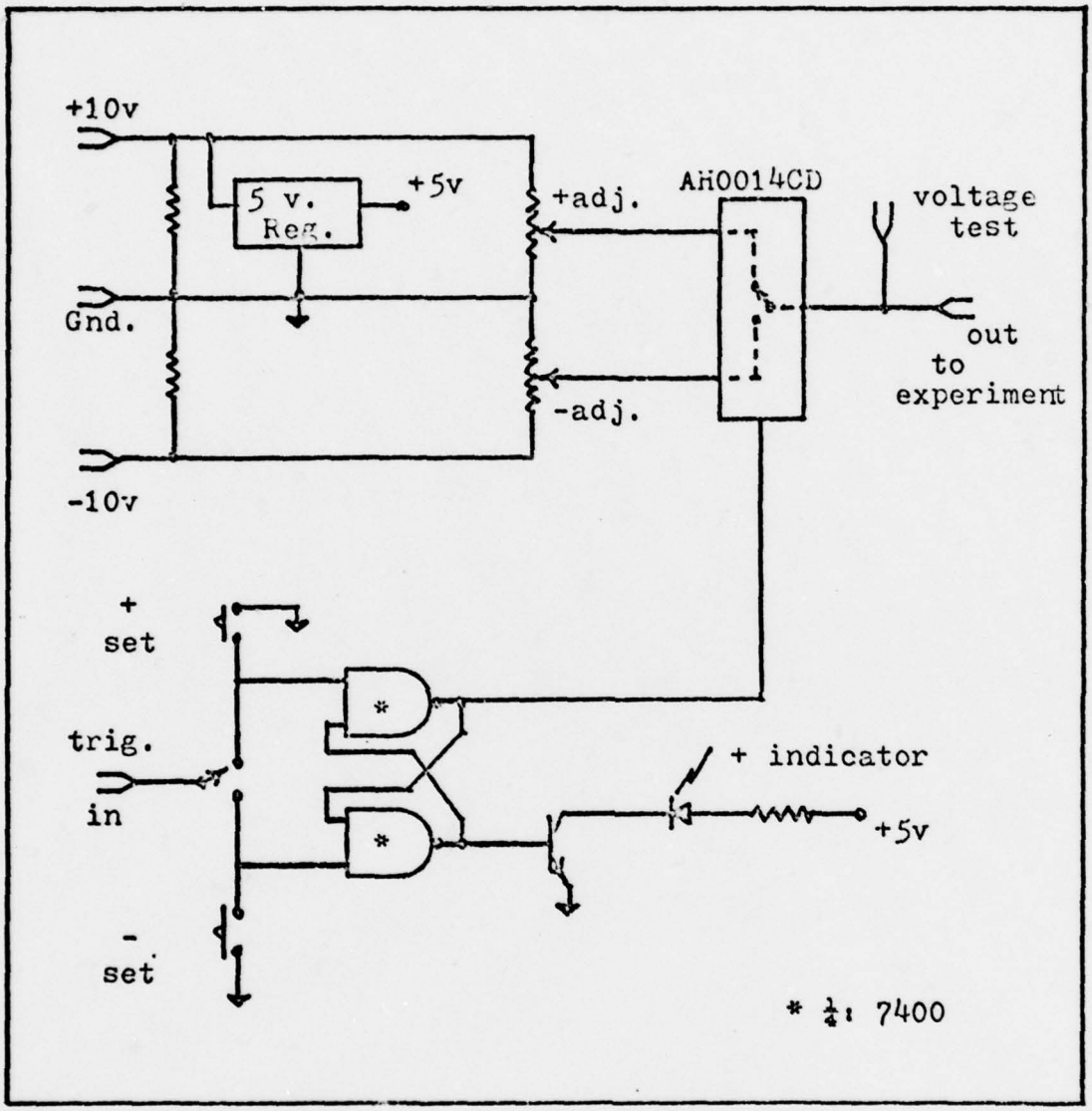

Fig. 3-2. Schematic of the trigger unit.

The digital section consists of the equipment connected directly to the HP-1B system bus (see Fig. 3-1). The bus is controlled by an HP 9825A calculator. An HP 9871A printer and an HP 9872A plotter provide the output of the digital section. Data are entered through an HP 3437A DVM. This voltmeter acts as an analog to digital converter and as the source of the trigger signal for the analog section. This voltmeter is programmed and its output read via the bus.

The temperature controller section consists of a Varian V-4540 temperature control and a separate Chromel-Alumel thermocouple. The temperature control works with a stream of gaseous nitrogen. The stream is first cooled in a bath of liquid nitrogen then reheated by a feedback controlled resistance heater to the desired temperature. The stream leaving the heater tube is constrained to flow around the sample by a shielded styrofoam insulating jacket. Since the sample is several millimeters from the end of the heater tube, its temperature is different than that of the gas stream in the tube. To accurately measure the sample temperature, a Chromel-Alumel thermocouple is attached with tape to the sample header. The output of the thermocouple is read by an HP 3455A DVM capable of 1 microvolt resolution. The thermocouple was calibrated in liquid nitrogen, and its corrected output converted to degrees Celsius by standard tables (Ref 6).

Sample Preparation

Samples used in this study were prepared by mounting them in TO-5 headers with conductive epoxy (Able Bond 36-2). A gold wire was then connected between the gate and the lead of the header using the same adhesive material. This procedure is necessary due to the fact that the normal bonding procedures, ultrasonic or thermal compression, cause severe damage to the sample. To verify that this procedure introduced no anomalies, the silicon reference sample was also prepared in this manner.

Procedure

The software developed for the calculator (see Appendix A) handles the data recording and processing. This leaves a very simple procedure for the operator. The voltage is adjusted using the controls on the trigger unit, then the temperature is selected using the temperature controller, and the device is biased into accumulation. After the temperature as measured by the thermocouple and the current as measured by the picoammeter are stable, the zero of the picoammeter is checked and the temperature recorded. The routine LONG READ is initiated causing the voltage step to be applied to the sample and the data to be recorded. A second reading is obtained from the thermocouple and the temperature average is computed. The data is then scaled and assembled into an array by the calculator. The array is composed of 500 ordered pairs (x,y) where x is the time

in seconds from t=0, and y is the current in Amperes at time x. Next, the routine PACK is called. It calculates the average and standard deviation of the current readings starting from x=10 and ending at x=25 seconds. PACK then adds the temperature in ^{o}K as a third parameter and stores this information in array B.

The above process is repeated until the temperature has been stepped across the desired range. A data output is then obtained as a plot (via routine PLOT B) or a listing (via routine PRINT B). The data may also be filed (using FILE B) on tape for future use. The output of PLOT B is the desired profile if the device behaves according to the theory of Simmons and Wei (Ref 3).

The digital system makes it possible to save even the raw data arrays (using routine FILE). This is useful in allowing some data to be saved and processed in varying ways without repeating the experiment.

IV. Results

Silicon Results

Reference measurements were made on a Si sample to provide a measure of confidence that the system functioned as planned. The sample was n-type Si with 76 nm of thermally grown oxide on a (111) surface and a .01824 cm^2 Au dot as a gate electrode. Two measurements were made on this sample using different bias changes. The first (Fig. 4-1) used a change of +5 to -5 volts. The second (Fig. 4-2) used a change of +8 to -7 volts. As predicted by the theory there was no appreciable difference in these results, and they closely matched the published data for density of states vs. energy (Ref 7:452). The data marked with an asterisk (*) are the result of a procedure used to detect dependence of the sample on bias history. This procedure will be explained when GaAs is discussed.

Figure 4-3 shows the results of the calculation of change in surface potential with energy. This calculation is used as a check on the validity of the energy scale. Since the maximum change in surface potential is less than the bias voltage change, the energy scale for Si is in fact as assumed in the theory.

Gallium Arsinide Results

The GaAs samples studied were provided by B. Bayraktaroglu. These samples are native oxide MOS devices

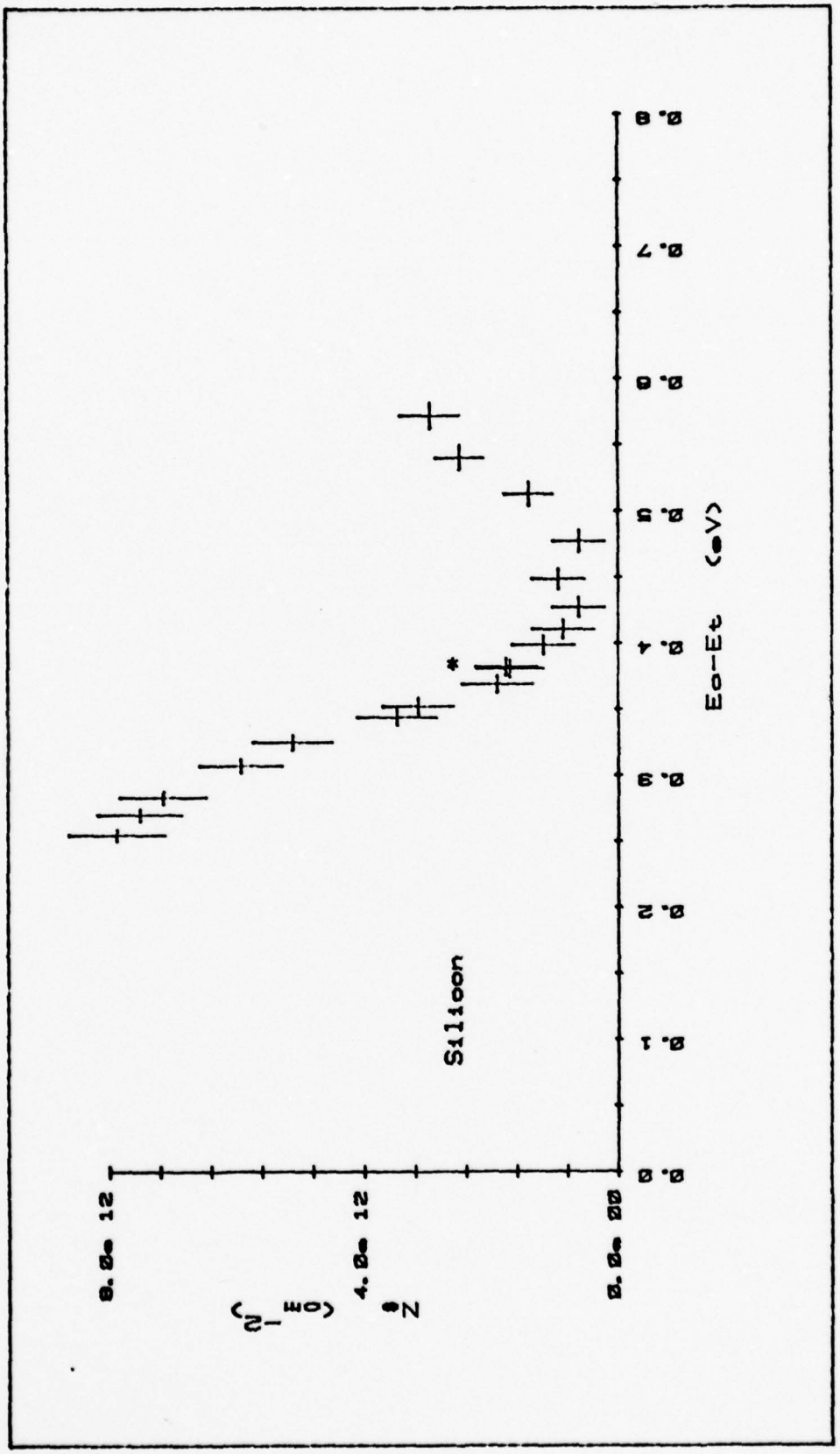

Fig. 4-1 Data for Si using a +5 to -5 volt bias change.

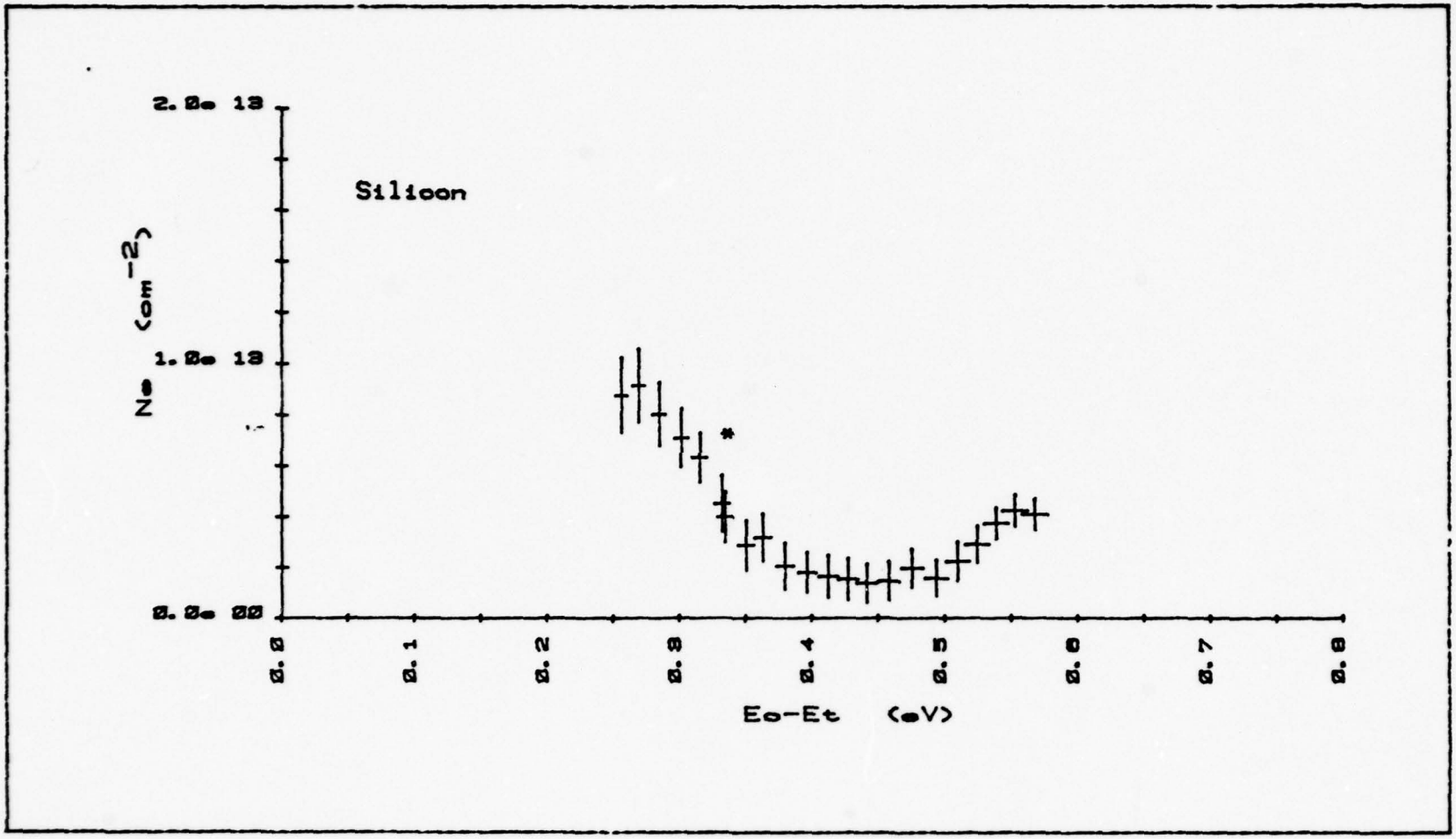

Fig. 4-2 Data for Si using a +8 to -7 volt change.

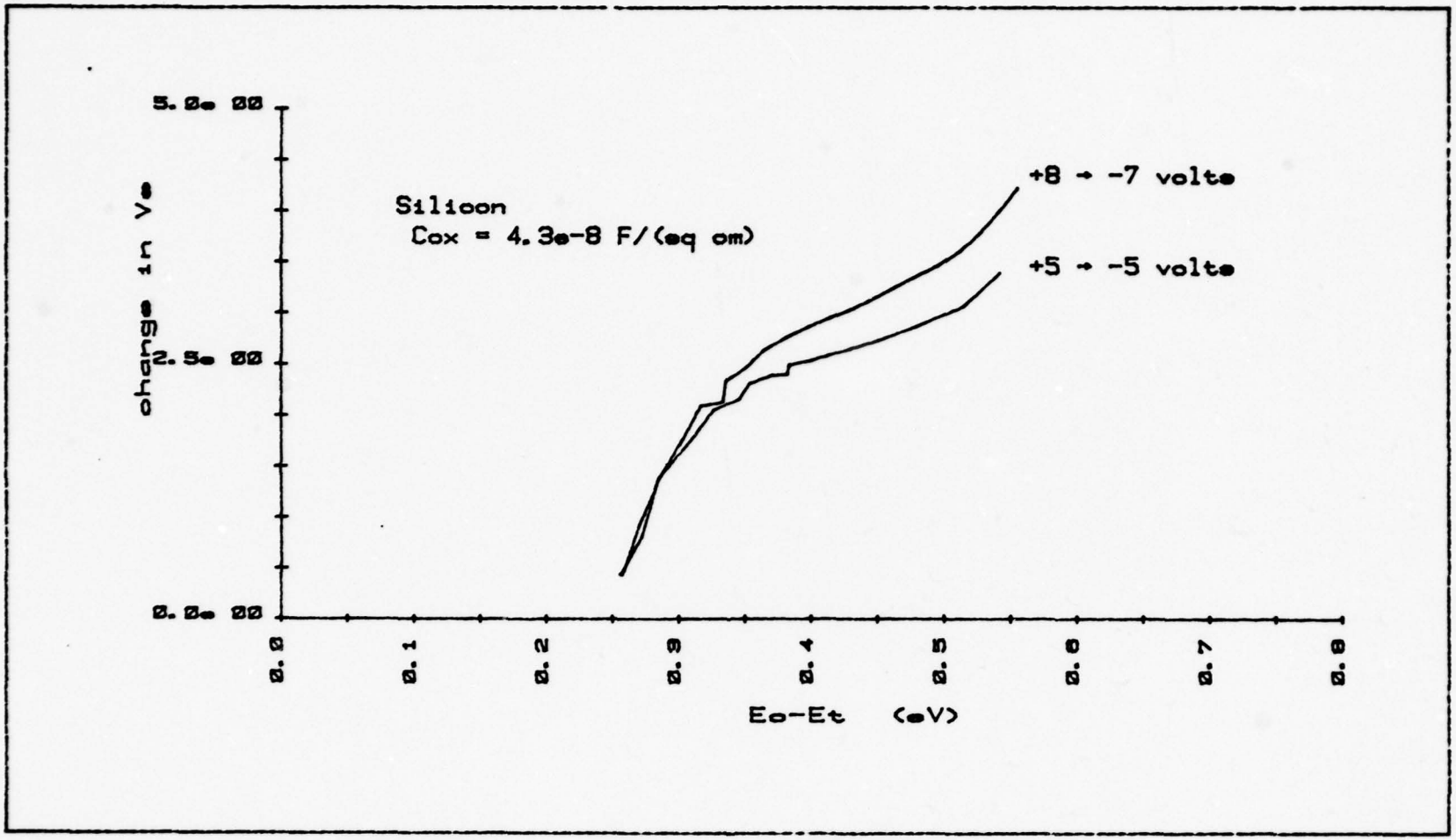

Fig. 4-3 Calculated change in surface potential for Si data.

produced by anodic oxidation. The substrate is N-type GaAs with a doping of 10^{17} impurities per cm^3. The oxide layer is 100 nm thick, and the gate is a .00051 cm^2 Al dot. Two versions of this device were studied. Sample B3A was not annealed and sample B4A was annealed at 350° C for 15 minutes. The results from the basic experiment are shown in Figs. 4-4,5. The data point marked with the asterisk is again the result of the procedure used to detect dependence of the sample on bias history. The procedure was to cool the sample to the lowest temperature to be used, then warm it in steps. At each step a measurement was made. A final measurement was made at a lower temperature. If there is little or no dependence on bias history the last point will fall on the curve obtained during the heating cycle. This is the case for the Si data. In the case of sample B4A however, the last point falls well away from the rest indicating a dependence of the characteristics of the sample on the bias history. Figures 4-6,7 depict the results of two more measurements, first with a larger bias change (+2.5 to -3 volts), then with the original +2 to -2 volt change. These results support the idea that the bias and bias history affect the characteristics of this sample.

The plots of change in surface potential vs. energy given in Fig. 4-8 for sample B4A show clearly that the energy scale is in error. They indicate a maximum change in surface potential greater than the applied bias change. This is not actually possible, but the calculations can

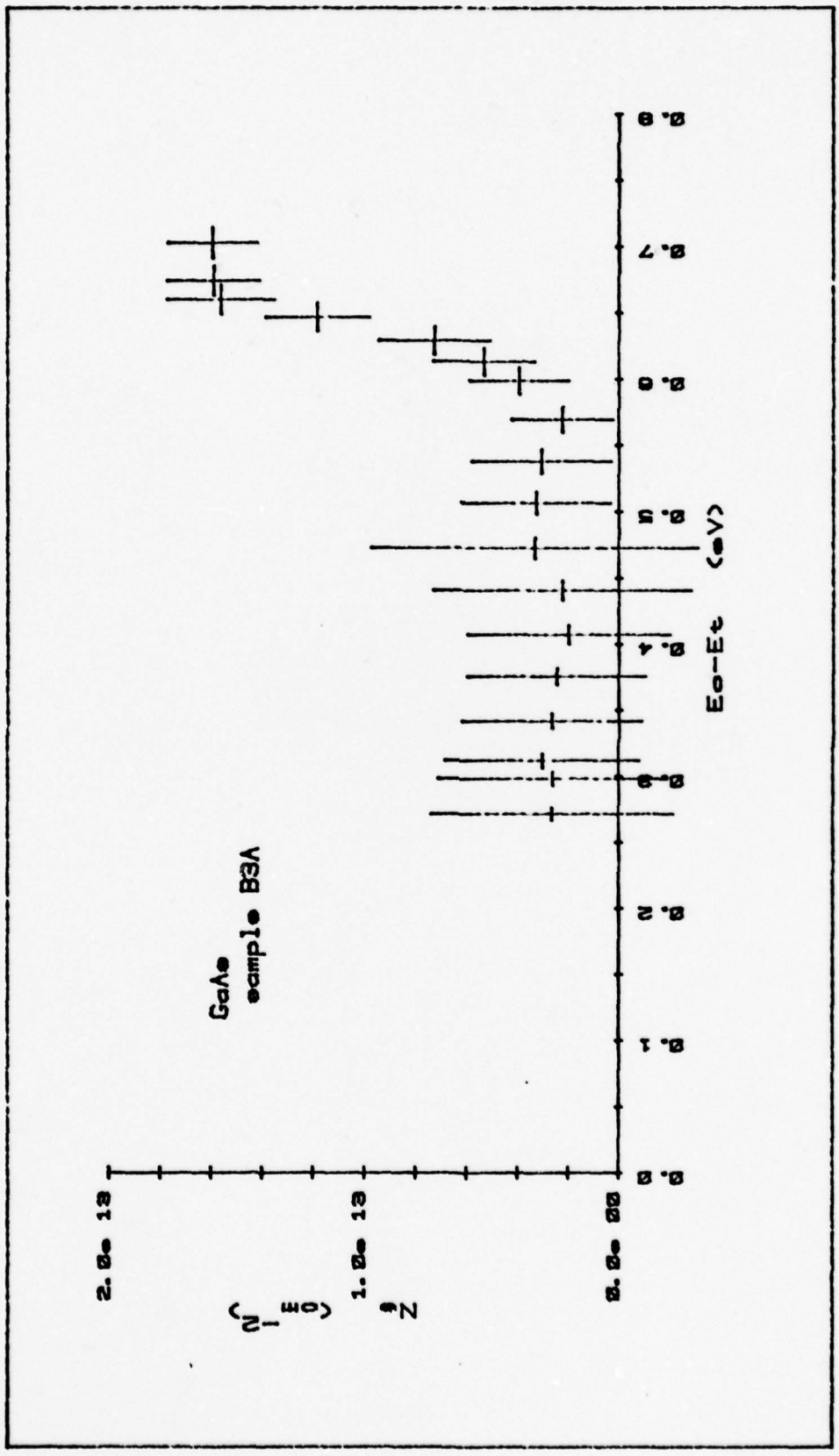

Fig. 4-4 Unannealed GaAs data.

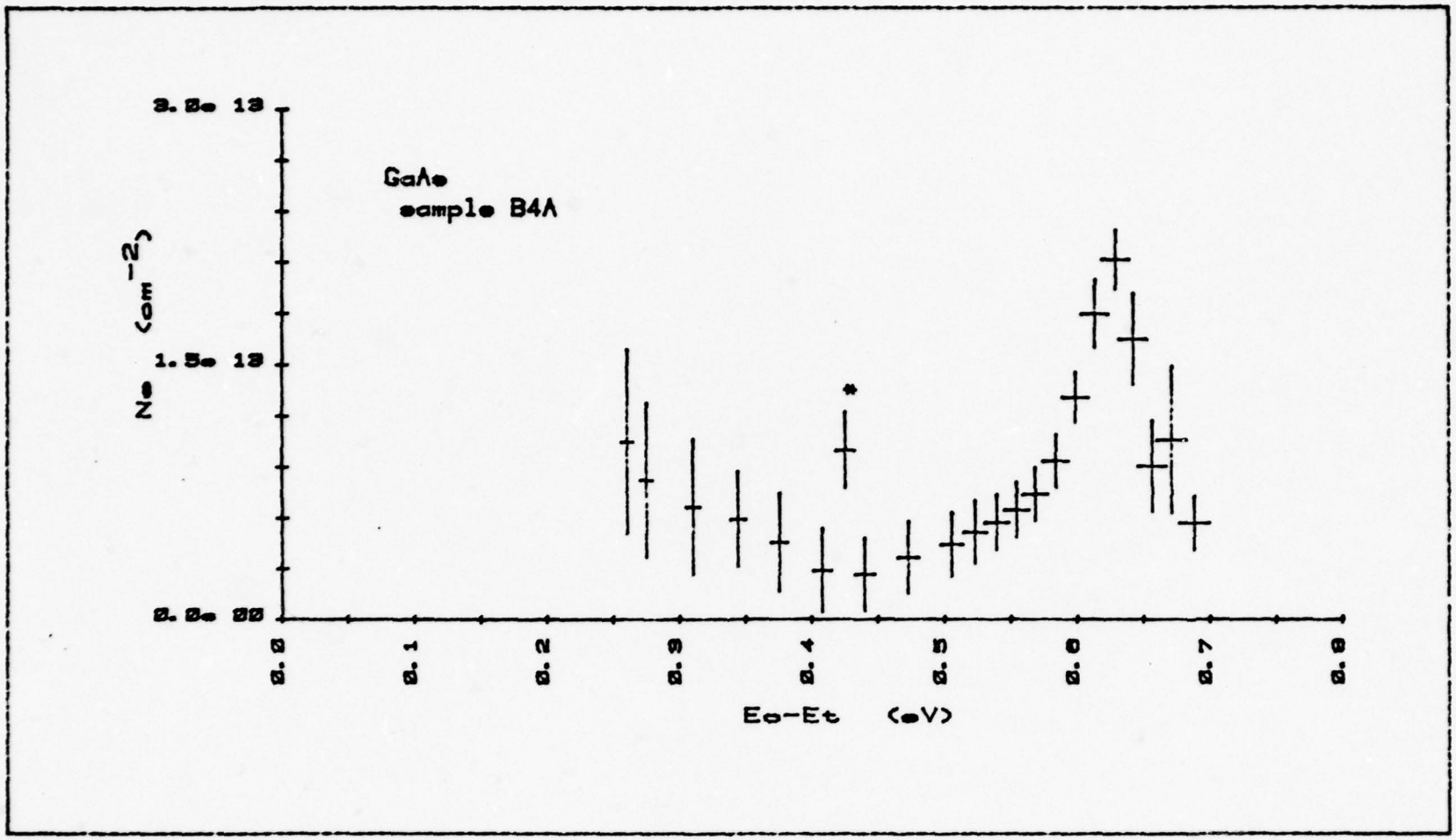

Fig. 4-5 Annealed GaAs data using +2 to -2 volt bias change.

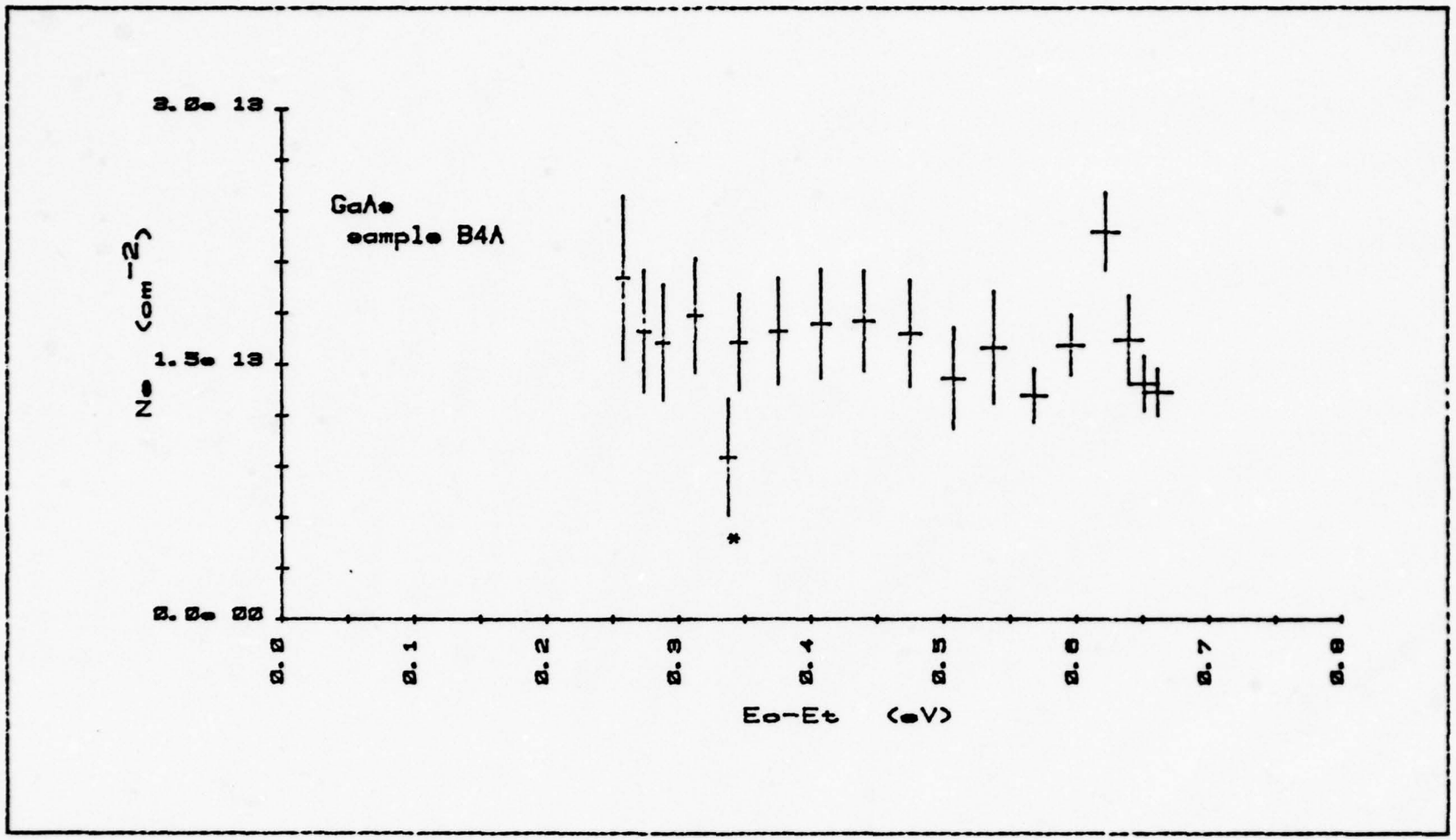

Fig. 4-6 Annealed GaAs data using +2.5 to -3 volt bias change.

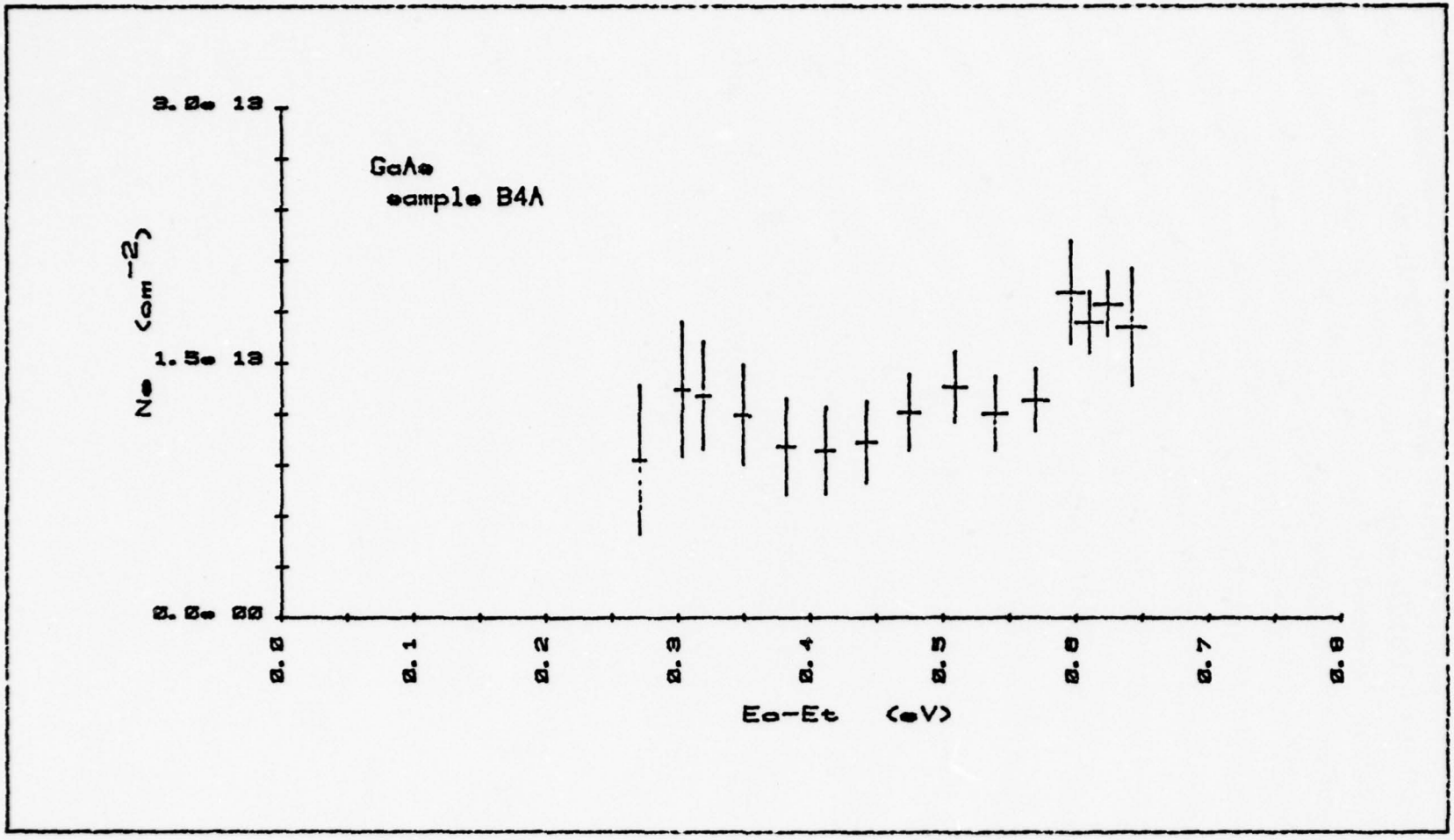

Fig. 4-7 Annealed GaAs data using +2 to -2 volt bias change.

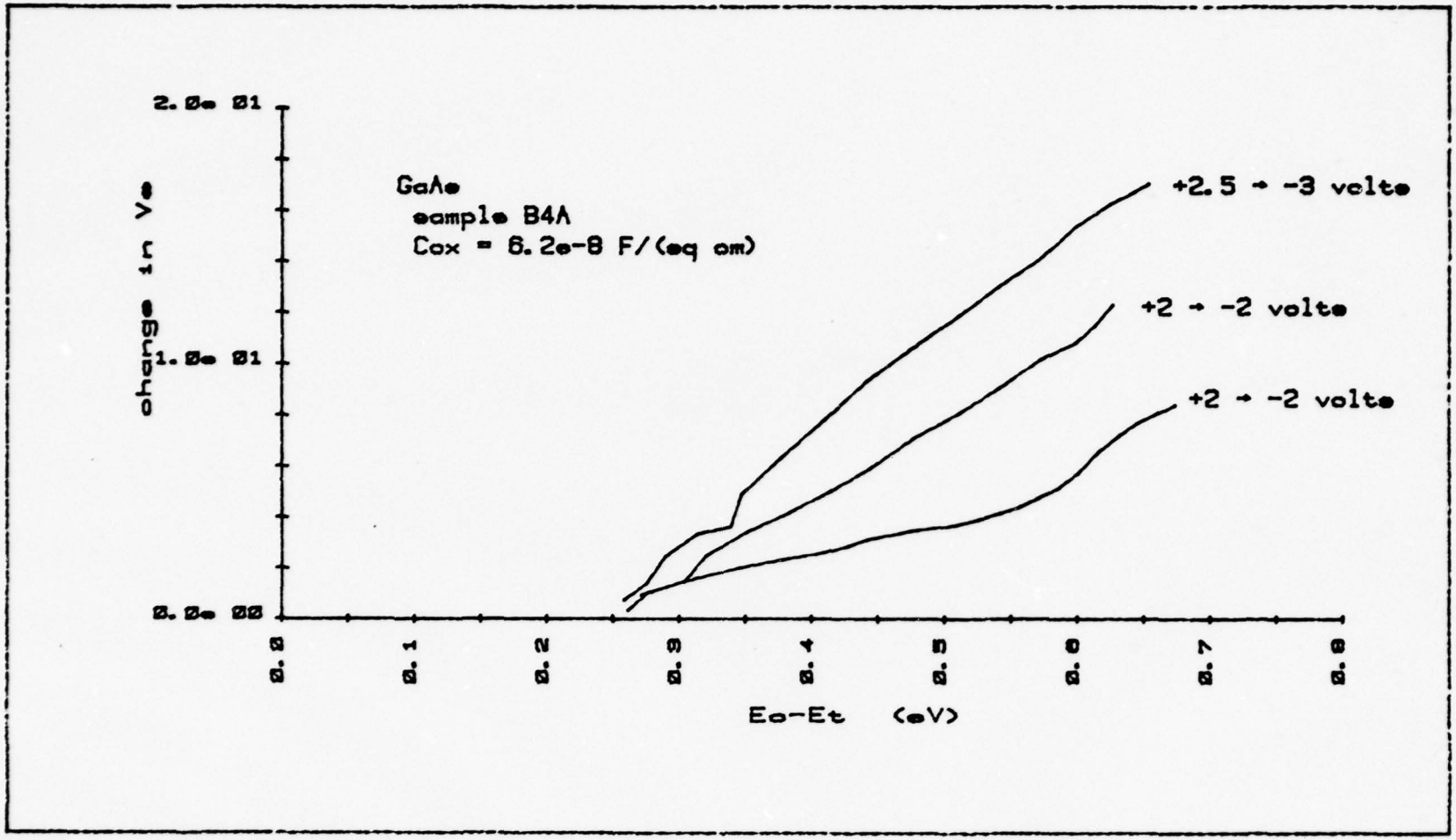

Fig. 4-8 Calculated change in surface potential plot for GaAs.

be expected to give this indication if the energy range actually explored was smaller than the range assumed in the calculation.

Two more measurements were made to clarify this dependence on bias history. Figure 4-9 shows the results of biasing the sample B4A at -2 volts for more than 24 hours at room temperature, then cooling it for the measurement while maintaining a bias of -3 volts. The bias change for the experiment was +3 to -3 volts. Figure 4-10 shows the results of 3 hours under +3 volts bias at room temperature and the subsequent cooling of the sample for the measurement while it was under +3 volts bias. The region of special interest in Figs. 4-9, 10 lies between .35 and .5 eV. In Fig. 4-9 the negative bias has caused a broad maximum in the density of states to occur in this region. In contrast, Fig. 4-10 displays a minimum in the region of interest due to the action of the positive bias.

The most plausible explanation of this behavior is that there exists a large density of mobile charges in the oxide which migrate to or away from the semiconductor-oxide interface under the influence of the bias field. Moreover, since these charges appear to leave the interface, i.e. become less effective in pinning the surface potential, under a positive bias, it appears that the majority are negatively charged. This contrasts sharply with the familiar situation in Si where interface charges are predominantly positive. Given the lack of stoichiometry in the oxide on GaAs, it

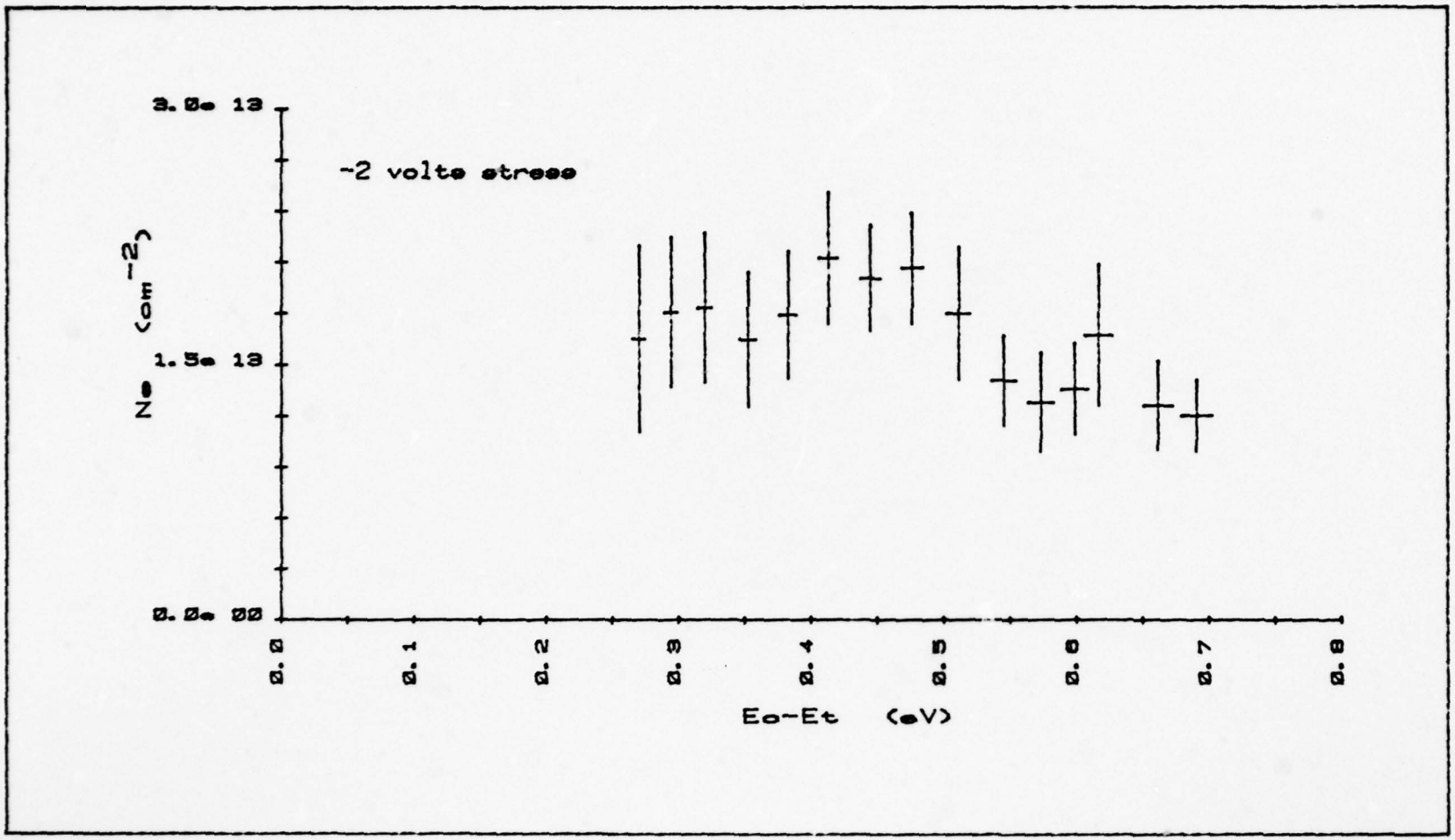

Fig. 4-9 Negative bias stress test.

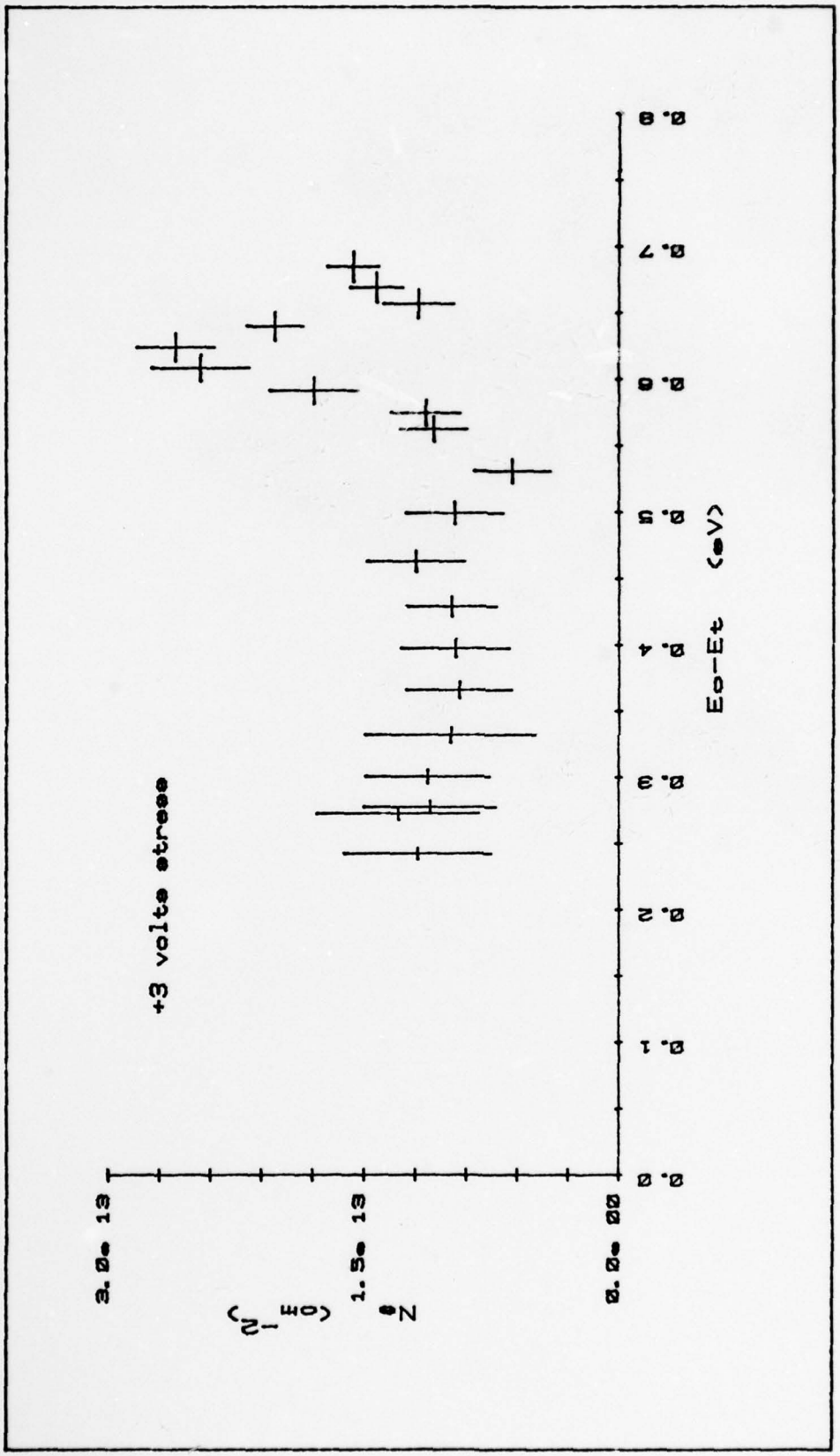

Fig. 4-10 Positive bias stress test.

may be that Ga^- or other ionic species introduced during anodization are responsible for this mobile charge.

In all of the density plots there is an indication of a large density of fixed states near the mid-gap energy level, and some of the results show fixed states near the conduction band.

V. Conclusions and Recommendations

Conclusions

This experiment is an improvement over the version used by Mar and Simmons. While the basic theory is the same, the implementation, especially the digital data processing, allows greater flexibility, and provides the ability to perform sophisticated data analysis very easily.

The experiment, as it is now implemented, provides a powerful tool with which to study GaAs MIS structures. The digital data processing provides the flexibility to easily vary the way the data is collected by changing such parameters as the sample rate. More importantly, the data can be analyzed quickly and accurately to yield more information. The error estimate represented by the standard deviation is one example of such an analysis. The very useful plots of change in surface potential vs. energy provide another example of this capability.

The results of measurements using this technique lead to several conclusions concerning the anodic oxide MIS device represented by Sample B4A.

1. There exist high densities of fixed trap states both near the conduction band and near mid-gap.

2. There exist large numbers of mobile charges in the oxide; when located at the oxide interface, they introduce trap states that lie, in energy, between the two peaks of

fixed trap state density.

3. Due to the large density of trap states, both mobile and fixed, the Fermi level is not able to move under applied bias as assumed in the basic theory.

4. The mobile trap states respond as if negatively charged, they are mobile at room temperature, and they lie, in energy, between the peaks of fixed trap density. These traps, due to both their concentration and their mobility make this oxide unsuitable for device application, since they would make MOS thresholds too large and unstable for useful device characteristics.

The results of the change in surface potential vs. energy plots indicate that the energy scale as plotted according to the theory is in error. The scale indicates a range of energy that is larger than the range actually explored. This means that the transient occupation function of the theory will have to be modified to produce a correct energy scale when used with samples that have a large density of interface and oxide trap states. It can also be noted that as the quality of anodic or other oxides improves to the point where device structures become practical, the difficulty introduced by large mobile charge densities will correspondingly decrease, making this measurement technique increasingly accurate and useful.

Recommendations

Based on the success of this experimental measurement it is recommended that:

1. The experiment be used to further study GaAs MOS structures,

2. The experiment be improved with the use of a temperature controller capable of cooling to a lower temperature,

3. The theory be improved to yield a more accurate conversion from time to energy in the presence of many trap states, specifically by incorporating a transient occupation function which more accurately reflects the actual mechanisms present in GaAs anodic oxides.

Bibliography

1. Hasegawa, H. and H. Hartnagel. "Anodic Oxidation of GaAs in Mixed Solutions of Glycol and Water." Journal of the Electrochemical Society, 123:713 (1976).

2. Mar, H. A. and J. G. Simmons. "Determination of the Energy Distribution of Interface Traps in MIS Systems Using Non-Steady State Techniques." Solid State Electronics, 17:131 (1974).

3. Simmons, J. G. and L. S. Wei. "Theory of Transient Emission Current in MOS Devices and the Direct Determination of Interface Trap Parameters." Solid State Electronics, 17:117 (1974).

4. Stannard, J. "Transient Capacitance in GaAs and InP MOS Capacitors." Journal of Vacuum Science Technology, 15 (July/August 1978).

5. Schuermeyer, F. and H. Hartnagel. "Electrical Analysis Methods for Passivated GaAs." Unpublished paper.

6. Handbook of Physics and Chemistry. Cleveland: The Chemical Rubber Publishing Co., 1962.

7. Sze, S. M. Principles of Semiconductor Devices. New York: Wiley Interscience, 1969.

Appendix A

Calculator Software

Introduction

The data collection and processing for this experiment was done with a Hewlett-Packard 9825A calculator. The String Variable-Advanced Programming (98210A), Matrix (98211A), and Plotter-General I/O-Extended I/O (98216A) read only memories were installed. The calculator has an integral magnetic tape cartridge to store program and data. Upon inspecting the instruction set for the tape cartridge, it became apparent that if large amounts of data or complex programs were to be used, the operation of the tape cartridge system would have to be as automatic as possible. A system program called TAPE MONITOR was written to do this. This system program and the program for the experiment were written in modules or states. This allowed the easy addition or deletion of program modules as new ideas were formulated and old ones discarded.

Variables and Conventions

To pass data between the modules some conventions were established. The following "r" variables were given special meaning:

r1 = current number of tape files

r2 = current track

r3 = current file

r4 = data array length/byte length for data or program

r5 = status variable

r6 = scale factor

r7 = scale factor

r8 = temporary storage

r9 = automatic mode indicator

r11 = the next usable program line after the experiment program

r12 = the next usable line of program after TAPE MONITOR

(r11 and r12 are used to link program modules from tape memory to calculator main memory)

r15, r16, r17, r18, and r19 are used in the CONVERT subroutines.

A string variable matrix and a numeric matrix are used to store the file tables needed in the system routines. F[50,4] is allocated as follows:

F[n,1] track number

F[n,2] file number

F[n,3] status where 2 is used and 0 is free

(F[1,3] is used to store r1)

F[n,4] absolute size of the file

F$[50,10] contains the names of the files. Each name can be up to 10 characters long.

String variables A$ and B$ are used to pass names and labels respectively.

A[500,2] is an array of ordered data pairs 500 pairs long. B[40,3] is an array or ordered data triples 40 triples long. The arrays A and B are used to transfer data from one module to another.

Each module is described separately in as much detail as its complexity warrants. Verbal descriptions and flow diagrams are used as needed to explain the listings.

System Program

The system program, TAPE MONITOR, is really more of a file manager, and is composed of modules that aid in using the tape cartridge memory. The first module (Figs. A-1,2) is an initialization and selection or directory state. It dimensions the arrays needed for the operation of the system modules in a manual mode. Two of the modules are vectors to the experiment program, DATA MANIPULATOR. These transfer control to the experiment program which retains control unless it is directed by the operator to return control to the system. The other modules all return control to the directory when they are in the manual mode. This distinction is made since MARK FILE and LOCATE FILE are capable of being used as subroutines, and in this automatic mode they return control to the calling routine.

PRINT TABLE and FREE FILE. The simplest of the system modules are PRINT TABLE and FREE FILE (Fig. A-3). Each of these does just what its name implies. PRINT TABLE prints a listing of the current status of the tape file. It finds

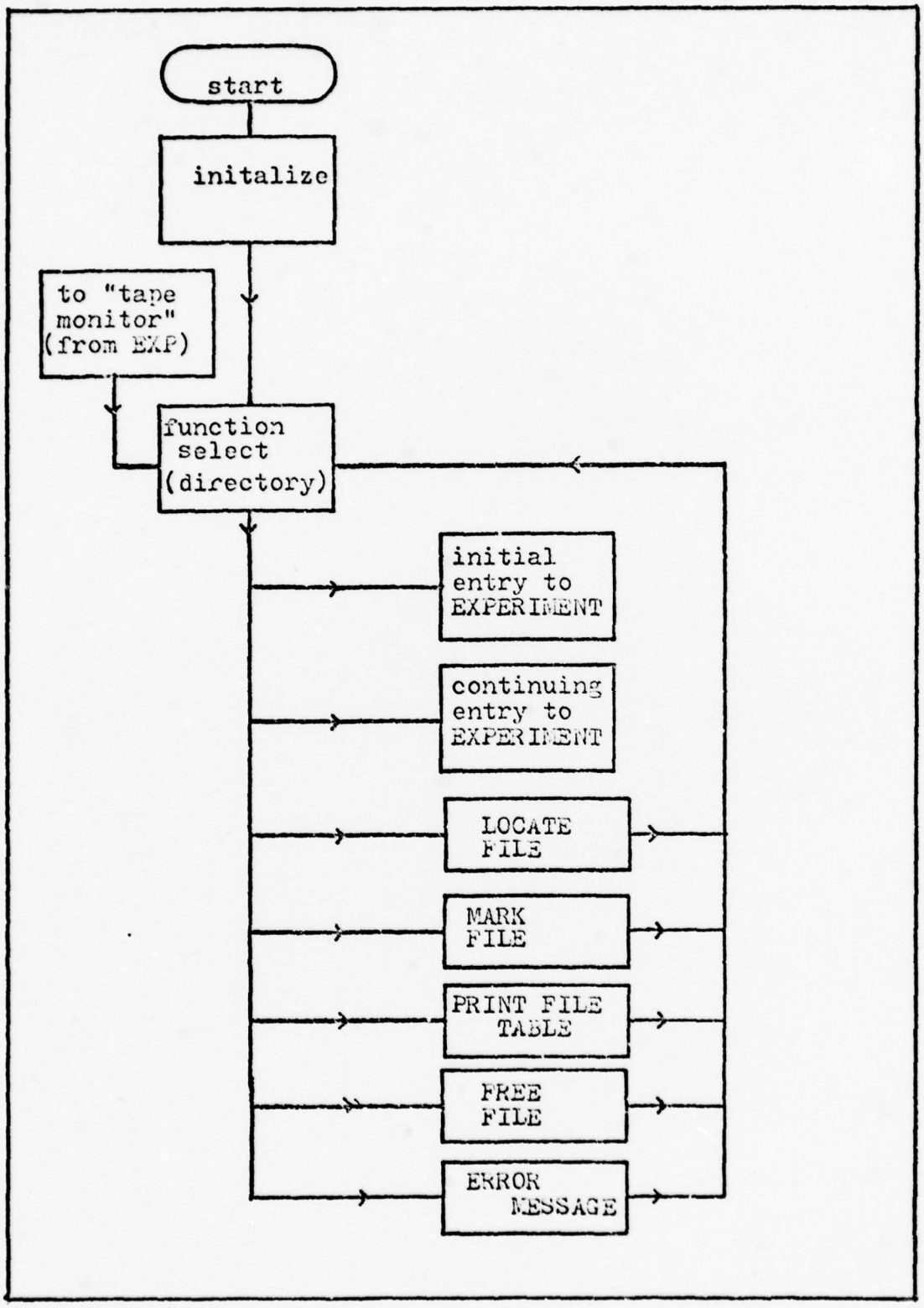

Fig. A-1 Tape Monitor flow diagram.

```
0: "Entry and Initialization":
1: dim F[50,4],F$[50,10],A$[10];trk 0
2: ldf 1,F[*];ldf 2,F$;F[1,3]→r1;72→r12
3: "Function Select State":
4: "Tape Control":ent "Enter the function code.",A$;cap(A$)→A$
5: 0→r9
6: if A$="LF";gto "LOCF"
7: if A$="M";gto "MARK"
8: if A$="PT";gto "PT"
9: if A$="EXP";trk 0;ldf 15,r12
10: if A$="EXPC";gto "EXPC"
11: if A$="FF";gto "free file"
12: dsp "TAPE CONTROL ERROR !!";beep;wait 2000;gto "Tape Control"
*15301
```

Fig. A-2 Tape Monitor listing.

```
14: "   print table routine  ":
15: "PT":wrt 702," ";wrt 702," "
16: fmt 2,5x,"NAME",5x,"TRK",5x,"FILE",5x,"Current Size",5x,z
17: fmt 3,"Abs size",5x,"Type",/
18: wrt 702.2;wrt 702.3
19: fmt 1,c10,3x,f5.0,3x,f5.0,9x,f5.0,7x,f5.0,6x,f5.0
20: for I=1 to r1;trk F[I,1];fdf F[I,2];idf r20,r20,r21,r22
21: wrt 702.1,F$[I],F[I,1],F[I,2],r21,r22,r20
22: next I;fmt 4,3/;wrt 702.4
23: gto "Tape Control"
*26755



65: "  FREE FILE STATE  ":
66: "free file":ent "What is the file name?",A$;cap(A$)→A$
67: for I=2 to r1
68: if A$=F$[I];gto "FF1"
69: next I
70: beep;dsp "  NO SUCH FILE !!";wait 3000;gto "Tape Control"
71: "FF1":" "→F$[I];0→F[I,2];trk 0;rcf 1,F[*];rcf 2,F$
72: gto "Tape Control"
*27130
```

Fig. A-3 Listing for PRINT TABLE and FREE FILE modules.

part of its information in F and F$, and finds the rest by using an "identify file" command in the calculator language. FREE FILE asks for the name of the file to be freed, then checks for its existence. If it exists, the file space is marked as free, and its name is erased. If no such file exists, an error message is displayed, and control is returned to the directory.

MARK FILE and LOCATE FILE. The next two states, MARK FILE and LOCATE FILE, are more complex. Each has two main flow paths. One path is used for the manual mode. It interacts with the operator. The other path is an automatic mode that operates as an invisible subroutine, that is, there is no interaction with the operator to identify that it is running. The flow diagrams are the easiest way to trace the flow through these routines. In the automatic mode A$ is assumed to have the file name, and r4 is assumed to have the proper length. In the automatic mode r9 must be set to 1.

MARK FILE looks for a free file long enough to accommodate the new file. If the space is not found, a new file is marked; the file table is updated and recorded; and the track and file numbers are passed using r2 and r3. If the space is found, the files are updated and recorded and the track and file numbers are passed. (See Figures A-4,5.)

LOCATE FILE finds the track and file numbers of any active file. If it is asked for a non-existent file, an error is indicated. When the file is found, the track and

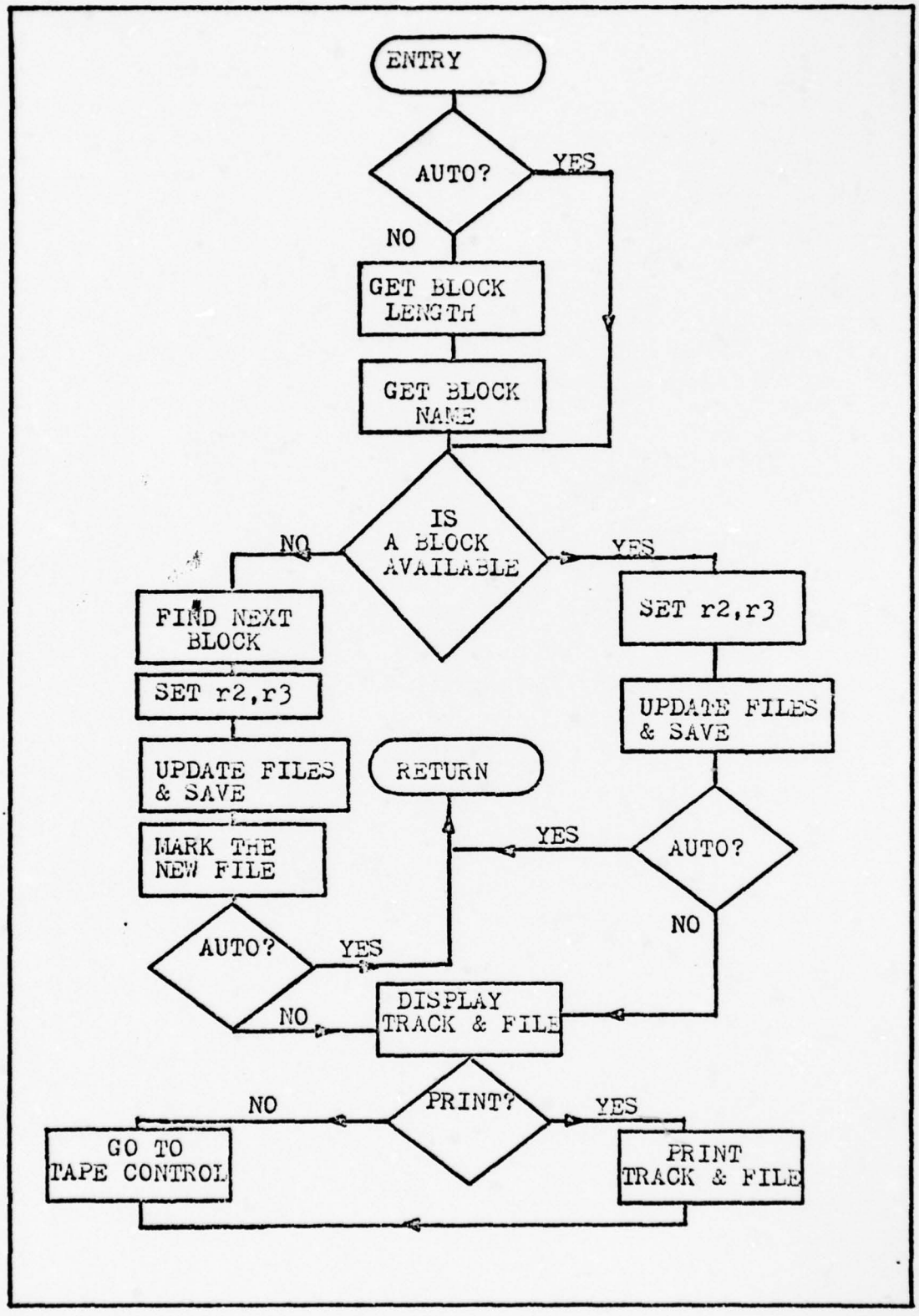

Fig. A-4 Flow diagram for MARK FILE.

```
23: "   MARK FILE STATE":
24: "MARK":if r9>0;jmp 3
25: ent "How large a file is it?",r4
26: ent "What is its name?",A$;cap(A$)→A$
27: for I=2 to r1
28: if F[I,3]=2;gto "m6"
29: if F[I,4]>=r4;gto "m0"
30: "m5":next I
31: r1+1→r1→r8
32: if r1>25;trk 1;1→r2
33: if r1<=25;trk 0;0→r2
34: r1-1→r5;F[r5,2]+1→r3
35: if r3>24;r3-25→r3
36: r2→F[r1,1];r3→F[r1,2];A$→F$[r1];2→F[r1,3];r4→F[r1,4]
37: trk 0;r1→F[1,3];rcf 1,F[*];rcf 2,F$;trk r2
38: fdf r3;mrk 1,r4;r4→F[r8,4]
39: "m7":if r9>0;ret
40: fxd 2;dsp "TRK  ",r2,"   FILE  ",r3;wait 5000
41: ent "Shall I print it?",r5
42: if r5;gso "m4"
43: gto "Tape Control"
44: "m4":spc ;prt F$[r8];prt "trk=",r2;prt "file=",r3;spc ;spc
45: ret
46: "m0":I→r8;2→F[I,3];trk 0;rcf 1,F[*]
47: F[I,1]→r2;F[I,2]→r3;A$→F$[I];rcf 2,F$;trk r2;gto "m7"
*18617
```

Fig. A-5 Listing for MARK FILE.

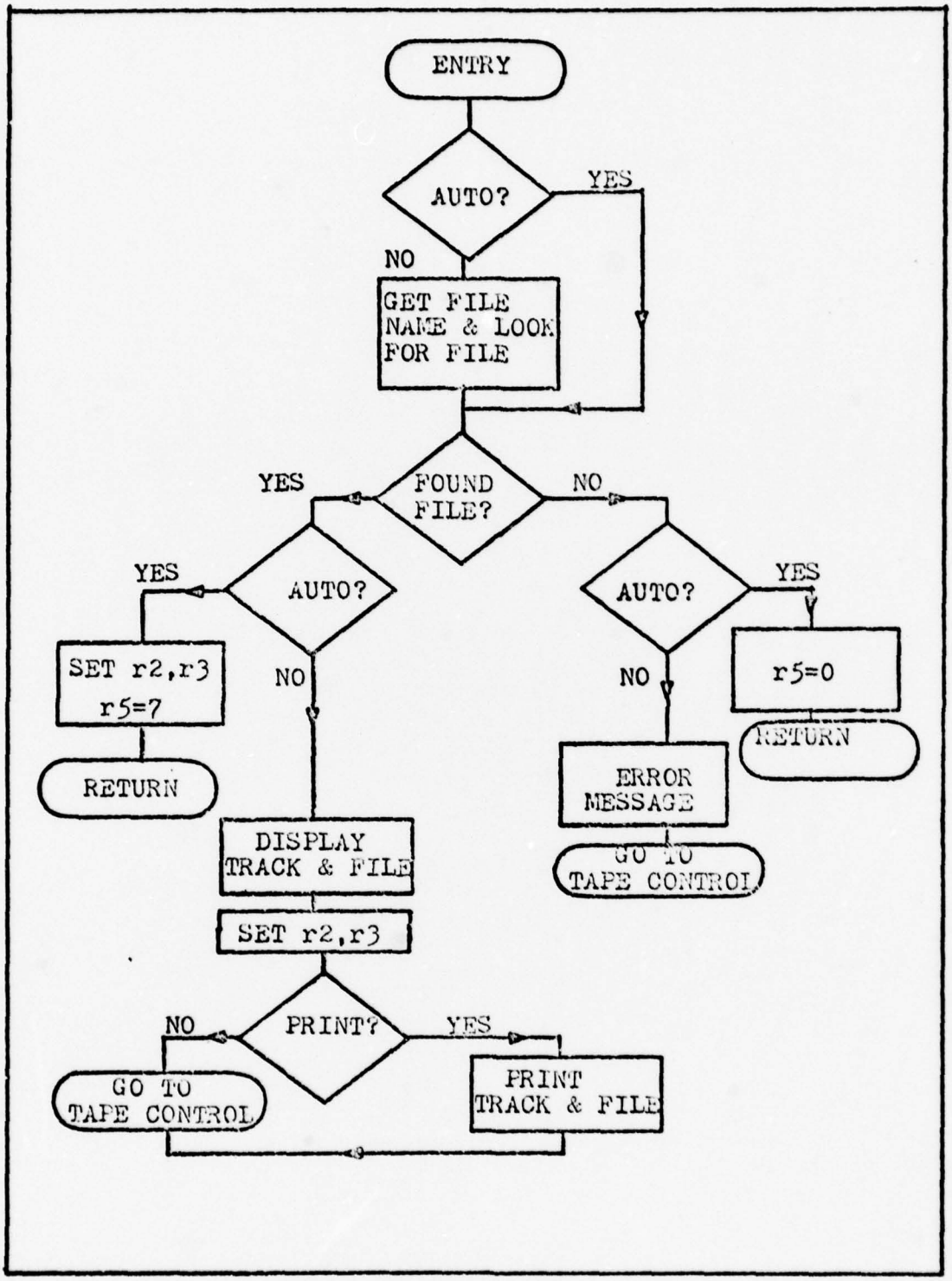

Fig. A-6 Flow diagram for LOCATE FILE.

```
48: "   LOCATE FILE STATE":
49: "LOCF":if r9>0;jmp 2
50: ent "What is the file name?",A$;cap(A$)→A$
51: for I=1 to r1
52: if A$=F$[I];if r9>0;jmp 7
53: if A$=F$[I];jmp 4
54: next I
55: if r9>0;0→r5;ret
56: dsp "NO SUCH FILE EXISTS !!";beep;wait 3000;gto "Tape Control"
57: fxd 0
58: dsp A$," is on TRK",F[I,1]," FILE",F[I,2];wait 10000
59: F[I,1]→r2;F[I,2]→r3;7→r5
60: if r9>0;ret
61: ent "  Shall I print  trk & file?",r5
62: if r5;prt " ";prt F$[I];prt "trk=",r2;prt "file=",r3;prt " "
63: gto "Tape Control"
*31112
```

Fig. A-7 Listing for LOCATE FILE.

file numbers are passed using r2 and r3 (See Figures A-6,7.)

Experiment Program

The experiment program, DATA MANIPULATOR, is also written in modules or states. Again they are loosely connected by a directory or selection state. One interesting feature is that some of the modules allocate memory in some way, and therefore have two entry points: an initial entry that allocates the memory, and another entry that bypasses these steps. This is necessary since the calculator does not allow an array to be dimensioned twice or a buffer to be declared twice. The initialization routine is one of these two-entry routines.

The selection state (Figs. A-8,9) has a vector to allow control to be transferred to the TAPE MONITOR. The other states all return control to the selection state in DATA MANIPULATOR. Each state will be considered separately.

TAPE READ. The TAPE READ module asks for the name of a data file. It expects the name of a file containing data that will fit into an array A dimensioned A[500,2]. There is a possibility of using this routine as a subroutine, but that is not done as the program is now written (Fig. A-10).

SCALE. The SCALE routine computes a conversion factor to convert the output of the DVM from volts to amperes. The routine interacts with the operator to obtain the range of the Keithley 417 picoammeter and uses the fact that full scale on the picoammeter is represented by 3 volts at the

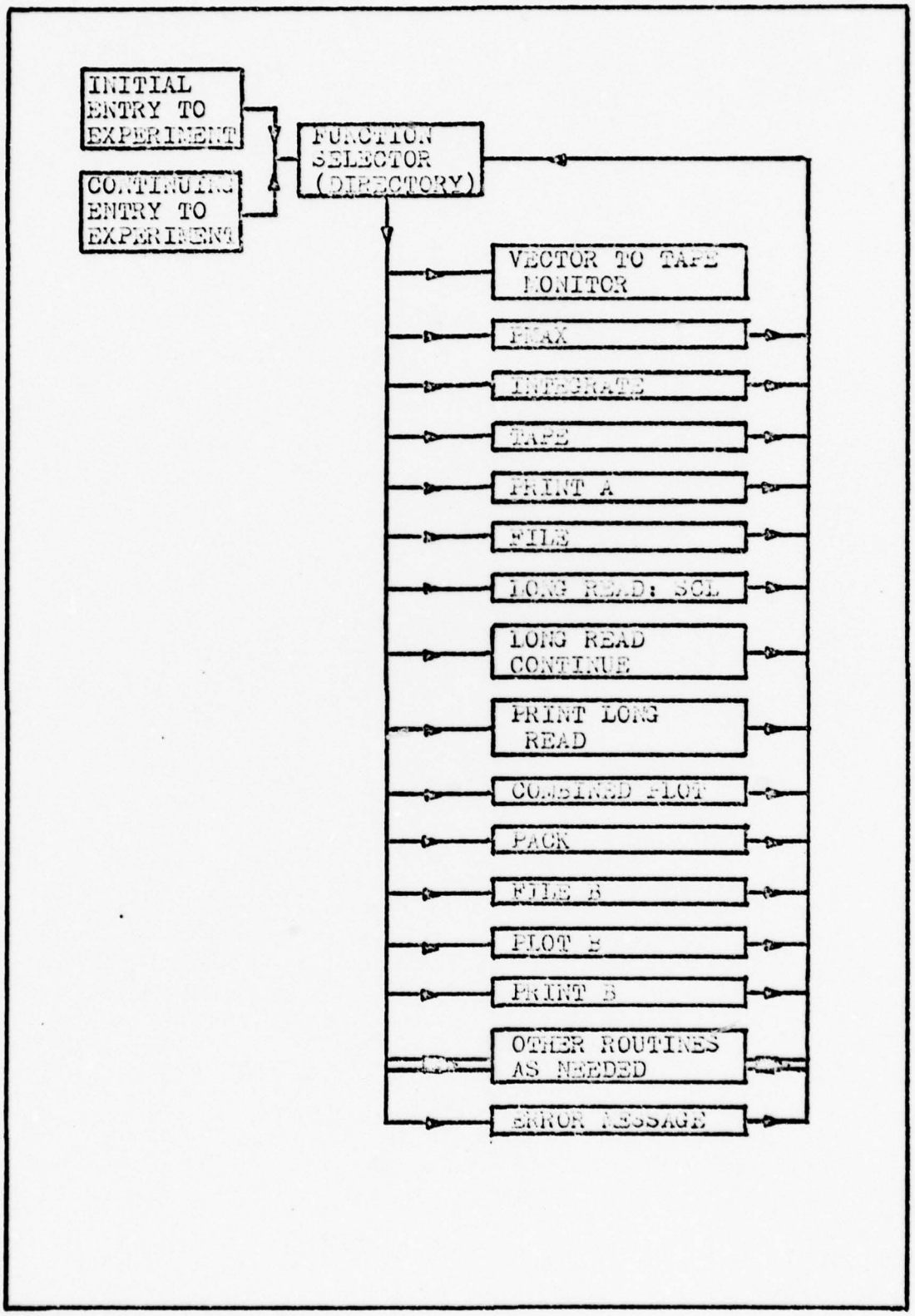

Fig. A-8 Flow diagram of the EXPERIMENT directory module.

```
72: "     DATA MANIPULATOR  ":
73: "  INITIALIZATION STATE":
74: dim X[2],Y[2],B$[30],A[500,2],B[40,3];239→r11
75: "  Input Choice State":trk 0;ldk 5
76: "EXPC":ent "Please select your OPTion",A$;cap(A$)→A$
77: if A$="INT";gto "INTEGRATE"
78: if A$="PMAX";gto "PMAX"
79: if A$="TM";gto "Tape Control"
80: if A$="TAPE";gto "TAPE"
81: if A$="PRINT A";trk 0;ldf 9,r11
82: if A$="FILE";gto "FILE"
83: if A$="LR";gto "Long Read"
84: if A$="PLR";gto "PLR"
85: if A$="LRC";gto "LRC"
86: if A$="COM P";trk 1;ldf 12,r11
87: if A$="PACK";gto "PACK"
88: if A$="FILE B";gto "FILE B"
89: if A$="PLOT B";gto "PLOT B"
90: if A$="PRINT B";gto "PRINT B"
91: beep;dsp "INVALID CODE    (C)";wait 2000;gto "EXPC"
*24008
```

Fig. A-9 Listing of the EXPERIMENT directory module.

```
103: "  Tape Read State  ":
104: "TAPE":ent "What is the name of the file?",A$;cap(A$)→A$
105: 500→r4;1→r9
106: gsb "LOCF"
107: if r5=0;beep;dsp "NO SUCH FILE";stp
108: trk r2;ldf r3,A[*]
109: if r9=3;ret
110: gto "EXPC"
*18151



118: "  Scale for Keithley 417 Picoammeter":
119: "SCL":ent "Picoammeter scale = ?",r8;r8/3→r8
120: for I=1 to r4;A[I,2]r8→A[I,2];next I
121: gto "EXPC"
*23189



111: "  Convert Subroutines  ":
112: "conv1":.1int(C/16)→r18;.01(frc(C/16)16)→r19;ret
113: "conv2":frc(C/16)16→r17;int(C/16)→r16
114: 10(frc(r16/2)2)→r16
115: int(C/32)→r15;frc(r15/2)2→r15
116: if r15=0;-1→r15
117: (r16+r17+r18+r19)r15→A[I,2];ret
*16598
```

Fig. A-10 Listings for TAPE, SCALE, and the CONVERT subroutines.

recorder output (Fig. A-10).

CONVERT. The CONVERT subroutines are used to convert the data from the packed format of the HP-3437A DVM to the normal calculator representation. The routines assume the DVM is set to the 10 volt range. If this is not true, a scaling step must be used in the calling routine to make the correction. These routines are used in conjunction with LONG READ, but can be used by other routines that operate the DVM in the packed mode.

They operate by dividing the numeric equivalent of the ASCII character by multiples of two, then using the fractional part or the integer part to form a string of "r" variables: r16, r17, r18, and r19. The sign is converted to a $\pm$ 1 which is assigned to r15. The expression, r15(r16+r17+r18+r19), is then the value of the reading.

LONG READ. LONG READ is the routine that programs the system DVM and allocates buffers for the data. When initiated it samples the voltage 500 times. Each sample is spaced .05 seconds apart. The routine then uses the CONVERT subroutines and a scale step to get the readings into volts as measured by the DVM. The routine then adds time increments to the A array. Exit is to the SCALE routine. (See Figure A-11.)

The A array produced by LONG READ and SCALE has the form of 500 ordered pairs. In each pair (x_n,y_n) x_n is the time in seconds from t=0 (due to a problem in representing ln) as a number, 0 is set as 1×10^{-6}sec.), and y_n is the value of

```
137: "Long Read":
138: dim C$[1016];500→r4
139: buf "cbuf",C$,3
140: "LRC":dsp "Long Read Ready !";stp
141: wrt 725,"D.05SN5000SE4SR2T1F2"
142: tfr 725,"cbuf",1000
143: rds("cbuf")→B;if B=-1;jmp 0
144: for I=1 to 500;2I→J;J-1→K;num(C$[J,J])→C
145: gsb "conv1"
146: num(C$[K,K])→C;gsb "conv2"
147: A[I,2]/10→A[I,2]
148: 1e-6+(I-1).05→A[I,1];next I
149: rdb("cbuf")→A;jmp rds("cbuf")=0
150: wrt 725,"T3";beep;gto "SCL"
*29871
```

Fig. A-11 Listing for LONG READ.

the current measured at time x_n.

FILE. FILE is the routine that allows the operator to save the raw data. It asks for the name to be assigned to the file and checks to see if the file name is already in existence. If the name is being used, it asks if the old file is to be updated. This prevents the inadvertent overwriting of data. When all these checks are complete, it marks a new file space to store the A array (or uses the old file in the case of an update), and files the data (Fig. A-12).

PLOT LONG READ. PLOT LONG READ produces a plot of the data in the array A. It plots both the I vs. t and the I·t vs. t curves. For the I·t vs. t curve the data is smoothed by an averaging function that uses the average of seven data points (three on each side of the point in question) as the value assigned at that point. PLOT LONG READ does not change any value in the A array. The routine scales and plots the axis automatically (Fig. A-13).

PACK. PACK is the module that creats the B array of processed data. This array is dimensioned B[40,3], meaning it is an array of 40 ordered triples. The B array has the following form: $B(x_n,y_n,z_n)$, such that n has a value from 1 to 40, and $B(x_1)$ is the number of the last triple to actually contain data, $B(y_1)$ is the area of the gate electrode in cm^2, and $B(z_1)$ is the value of the attempt to escape frequency for the sample. The rest of the array contains a summary of the results of up to 39 uses of

```
168: "FILE":beep;dsp "I intend to file A[*] on tape.";wait 2000
169: 1→r9;ent "what shall I name the file?",A$;cap(A$)→A$
170: gsb "LOCF"
171: if r5=7;jmp 4
172: 8000→r4;gsb "MARK"
173: 500→r4
174: trk r2;rcf r3,A[*];gto "EXPC"
175: ent "Is this an update of an old file?",r5
176: if r5;jmp -2
177: beep;dsp "I will need another name.";wait 1500;jmp -8
*20241
```

Fig. A-12 Listing of FILE.

```
141: "Plot Long Read":
142: "PLR":pclr;dsp "Prepare the plotter!  PLR";stp
143: A[1,1]*A[1,2]→r8
144: for I=1 to 500
145: if A[I,1]*A[I,2]>r8;A[I,1]*A[I,2]→r8
146: next I
147: gsb "SUB S"
148: pen# 1;scl 0,35,0,S
149: for I=2 to r4;plt A[I,1],A[I,2];next I;pen
150: flt 1;yax 0,S/10,0,S,5
151: 7→r6;3→r7;pen# 2
152: for I=r7+1 to r4-r7;0→r5
153: for J=-r7 to r7;A[I+J,1]A[I+J,2]+r5→r5;next J
154: plt A[I,1],r5/r6;next I;pen
155: fxd 0;pen# 1;xax 0,5,0,35,2
156: scl 0,100,0,100;plt 40,-15,1;csiz 2.5
157: lbl "time  (sec.)";plt -13,30,1;csiz 2.5,2,1,90
158: lbl "I  (Amps)";pen# 2;lbl "  I*t";plt 20,-25,1;csiz 3,2,1,0
159: pen# 1;ent "Label the plot",B$;lbl B$;pen#
160: gto "EXPC"
*29037
```

Fig. A-13 Listing of PLOT LONG READ.

```
178: "PACK":
179: if B[1,1]=0;ent "A=  sq cm",B[1,2];ent "nu=  ?",B[1,3];1→B[1,1]
180: 0→r6→r7;for I=201 to 500;A[I,2]A[I,1]+r6→r6
181: (A[I,1]A[I,2])^2+r7→r7;next I
182: B[1,1]+1→r20;r6/300→B[r20,1];r6^2→r6
183: √((r7-r6/300)/299)→B[r20,2]
184: ent "Temp. for this run =? deg C",T;T+273.15→B[r20,3]
185: r20→B[1,1]
186: if B[1,1]=39;dsp "B is full please file it.";wait 1500;gto "FILE B"
187: gto "EXPC"
*9590
```

```
188: "FILE B":dsp "Ready to file B[*]!";wait 1500;beep
189: 1→r9;ent "What shall I name the file?",A$;cap(A$)→A$
190: gsb "LOCF"
191: if r5=7;jmp 4
192: r4→T;960→r4;gsb "MARK"
193: T→r4
194: trk r2;rcf r3,B[*];gto "EXPC"
195: ent "Is this an update of an old B?",r5
196: if r5;jmp -2
197: beep;dsp "I will need another name.";wait 1500;jmp -8
*17109
```

Fig. A-14 Listing of PACK and FILE B.

LONG READ. Each $B(x_m,y_m,z_m)$ where m varies from 2 to $B(x_1)$ contains the following data: $B(x_m)$ is the average I·t value for the measurement, $B(y_m)$ is the sample standard deviation of the values that went into the average computed for $B(x_m)$, and $B(z_m)$ is the temperature in ^{o}K of the sample during the measurement.

After calculating and assigning the values as mentioned above, PACK then checks to see if the B array is full. If it is, PACK asks that the array be filed and exits to FILE B. If the B array is not full PACK exits to the selection state. (Fig. A-14)

FILE B. FILE B does for the B array exactly what FILE does for the A array, files it on tape (Fig. A-14).

PRINT B. PRINT B produces a listing of a B array. It uses SUB A to find the array and put it into main memory, then the routine outputs the listing to the printer (Fig. A-15).

PLOT B. PLOT B is the routine that plots the B array in the form of density of states vs. energy. It uses SUB A to locate the array and put the array into main memory, then it uses the equations presented in the theory to convert the I·t information into the needed form. Error bars indicating one standard deviation above and below the value are added. The plot is automatically scaled and the axis drawn and labeled. PLOT B allows more than one set of data to be plotted on the same axis for easy comparison (Fig. A-16).

```
215: "PRINT B":dsp "PRINT B Ready.";wait 1500
216: gsb "SUB A"
217: ent "Title the data.",B$
218: fmt 1,/,/,/,10x,c,/,5x,"Ave I*t",6x,"ST.Dev",6x,"Temp.",/
219: wrt 702.1,B$
220: fmt 2,3x,e9.2,3x,e9.2,3x,f9.2
221: for I=2 to B[1,1]
222: wrt 702.2,B[I,1],B[I,2],B[I,3]
223: next I
224: fmt 3,8x,"dot area =",f9.5,"sq cm",/,8x,"nu =",e9.2
225: wrt 702.3,B[1,2],B[1,3]
226: gto "EXPC"
*24032
```

Fig. A-15 Listing of PRINT B.

```
188: "PLOT B":dsp "PLOT B ready";stp
189: gsb "SUB A"
190: 1.602e-19→Q;8.62e-5→K
191: B[2,1]+B[2,2]→r8
192: for I=2 to B[1,1]
193: if B[I,1]+B[I,2]>r8;B[I,1]+B[I,2]→r8;I→r10
194: next I
195: B[1,2]→A;B[1,3]→V;B[r10,3]→T
196: r8/KQTA→r8
197: gsb "SUB S"
198: pclr;scl 0,.8,0,S;pen# 1;fxd 1;csiz 2;xax 0,.05,0,.8,2
199: flt 1;yax 0,S/10,0,S,5
200: csiz 2.5;plt .35,-.2S,1;lbl "Eo-Et  (eV)"
201: csiz 2.5,2,1,90;plt -.1,.4S,1;lbl "Ns  (cm";iplt -.01,0,1;lbl "-2"
202: iplt .01,0,1;lbl ")"
203: B[1,2]→A;B[1,3]→V
204: for I=2 to B[1,1];B[I,3]→T
205: KTln(10V)→r21;KTln(25V)→r22
206: (B[I,1]+B[I,2])/QKTA→r7;(B[I,1]-B[I,2])/QKTA→r8
207: B[I,1]/QKTA→r23
208: plt r21,r23,1;plt r22,r23,2;pen
209: plt (r21+r22)/2,r7,1;plt (r21+r22)/2,r8,2;pen
210: next I
211: ent "Is there more data?",r5
212: if r5=0;pen# ;gto "EXPC"
213: gsb "SUB A"
214: jmp -11
*18273
```

Fig. A-16 Listing of PLOT B.

SURFACE POTENTIAL PLOT. SURFACE POTENTIAL PLOT is the module that plots the change in surface potential as a function of energy by integrating the charge represented by the measured trap states and dividing by the oxide capacitance in Farads per cm^2. This routine uses parts of the A array as temporary storage. The data is taken from a B array located by SUB A, sorted and integrated by SUB B, and plotted by SUB C. The scale is automatically set with the help of SUB S. Axes are drawn that can be used with more than one set of data points. (Figs. A-17, 18, 19, 20)

Operation

The system as a whole is planned to be self-prompting and uncomplicated to use. Once the various elements of the experimental apparatus are connected, the tape cartridge containing the programs and data is inserted into the calculator. The commands, ldp 11 [EXECUTE] , are given to the system.

The tape will be accessed, and the system program, TAPE MONITOR, will be loaded and initiated. The calculator will respond with:

" Enter the function code. "

The list below provides the function codes for the system modules.

PRINT TABLE	PT
FREE FILE	FF
MARK FILE	M

```
227: "SPP":dsp "SURFACE POTENTIAL PLOT STATE";stp
228: 1.602e-19→Q;8.62e-5→K;ina A
229: gsb "SUB A"
230: gsb "SUB B"
231: A[41,2]→r8
232: for I=1 to r6-1;if A[40+I,2]>r8;A[40+I,2]→r8
233: next I
234: gsb "SUB S"
235: scl 0,.8,0,S
236: csiz 2;pen# 1;fxd 1;xax 0,.05,0,.8,2
237: flt 1;yax 0,S/10,0,S,5
238: csiz 2.5;plt .355,-.2S,1;lbl "Eo-Et  (eV)"
239: csiz 2.5,2,1,90;plt -.1,.4S,1;lbl "change in Vs"
240: gsb "SUB C"
241: ent "Is there any more data?",r5
242: if r5=0;gto "EXPC"
243: gsb "SUB A"
244: gsb "SUB B"
245: gsb "SUB C"
246: jmp -5
*13852
```

Fig. A-17 Listing of SURFACE POTENTIAL PLOT.

```
247: "SUB A":ent "On what file is the data?",A$;cap(A$)→A$
248: if A$=" ";jmp 4
249: 1→r9;gsb "LOCF"
250: if r5=0;beep;dsp "NO SUCH FILE";wait 1500;jmp -3
251: trk r2;ldf r3,B[*]
252: ret
*13569
```

```
276: "SUB S":int(10^frc(log(r8))+1)*10^int(log(r8))→S;ret
*5165
```

Fig. A-18 Listing of SUB A and SUB S.

```
253: "SUB B":0→r10
254: for I=2 to B[1,1]-1
255: if B[I,3]<=B[I+1,3];jmp 5
256: B[I,3]→r8;B[I+1,3]→B[I,3];r8→B[I+1,3]
257: B[I,2]→r8;B[I+1,2]→B[I,2];r8→B[I+1,2]
258: B[I,1]→r8;B[I+1,1]→B[I,1];r8→B[I+1,1]
259: 1→r10
260: next I
261: if r10=1;0→r10;jmp -7
262: B[1,1]→r6;B[1,2]→A;B[1,3]→V
263: for I=2 to r6;B[I,3]→T
264: KTln(V17.5)→A[I-1,1]
265: B[I,1]/QKTA→A[I-1,2]
266: next I
267: ent "C oxide=?  F/sq cm",C
268: 0→r3
269: for I=2 to r6
270: (A[I-1,2]+A[I,2])/2*(A[I,1]-A[I-1,1])+r8→r8
271: r8Q/C→A[39+I,2]
272: next I;ret
*4360
```

Fig. A-19 Listing of SUB B.

```
273: "SUB C":pen# 1;for I=1 to r6-2
274: plt A[I,1],A[I+40,2]
275: next I;pen;pen# ;ret
*23315
```

Fig. A-20 Listing of SUB C.

LOCATE FILE	LF
initiate the experiment	EXP
continue the experiment	EXPC

Type the code then press [CONTINUE].

If the code selected was EXP, then the tape will again be accessed and DATA MANIPULATOR will be loaded into memory and initiated. The display will now be:

" Please select your option. "

The list below provides the option codes for the experiment modules.

vector to TAPE MONITOR	TM
TAPE	TAPE
FILE	FILE
PRINT A	PRINT A
LONG READ	LR
continue LONG READ	LRC
PLOT LONG READ	PLR
PACK	PACK
PLOT B	PLOT B
PRINT B	PRINT B
SURFACE POTENTIAL PLOT	SPP

In any of the routines when data is required, the system provides a prompt. For questions requiring a yes or no type answer the system expects a "1" for a yes and a "0" for a no.

The calculator system and the software described here are in the custody of Mr. John Blasingame, AFAL/DHR, Wright-Patterson Air Force Base, Ohio 45433.

VITA

Martin John Biancalana was born on 3 September 1947 in Chicago, Illinois. He graduated from York Community High School in Elmhurst, Illinois and continued his education at the University of Illinois in Urbana-Champaign. He received a B.S. degree in Physics from the College of Liberal Arts and Sciences in 1969. Upon graduation he enlisted in the Air Force and after completion of technical training, served as a Precision Measurement Specialist at Incirlik CDI, Turkey. On returning to the United States, he earned a commission through OTS, and was assigned to the 90th Strategic Missile Wing, F. E. Warren AFB, Wyoming. Here he served as a Combat Targeting Team Chief, Instructor Team Chief, Quality Control Officer, and as OIC of Field Supervision until entering the School of Engineering, Air Force Institute of Technology, in June of 1976. He can be located at:

700 Cherry Street

Rome, New York 13440.

UNCLASSIFIED
SECURITY CLASSIFICATION OF THIS PAGE (When Data Entered)

REPORT DOCUMENTATION PAGE		READ INSTRUCTIONS BEFORE COMPLETING FORM
1. REPORT NUMBER AFIT/GE/EE/78-18	2. GOVT ACCESSION NO.	3. RECIPIENT'S CATALOG NUMBER
4. TITLE (and Subtitle) ELECTRICAL CHARACTERIZATION OF GALLIUM ARSINIDE ANODIC OXIDES USING ISOTHERMAL DIELECTRIC RELAXATION CURRENT		5. TYPE OF REPORT & PERIOD COVERED MS Thesis 6. PERFORMING ORG. REPORT NUMBER
7. AUTHOR(s) Martin J. Biancalana Capt.		8. CONTRACT OR GRANT NUMBER(s)
9. PERFORMING ORGANIZATION NAME AND ADDRESS Air Force Institute of Technology (AFIT-EN) Wright-Patterson AFB, Ohio 45433		10. PROGRAM ELEMENT, PROJECT, TASK AREA & WORK UNIT NUMBERS Project 2305-R1-80
11. CONTROLLING OFFICE NAME AND ADDRESS Electronic Research Branch Air Force Avionics Laboratory		12. REPORT DATE December 1978 13. NUMBER OF PAGES 78
14. MONITORING AGENCY NAME & ADDRESS(if different from Controlling Office)		15. SECURITY CLASS. (of this report) Unclassified 15a. DECLASSIFICATION/DOWNGRADING SCHEDULE

16. DISTRIBUTION STATEMENT (of this Report)

Approved for public release; distribution unlimited

17. DISTRIBUTION STATEMENT (of the abstract entered in Block 20, if different from Report)

18. SUPPLEMENTARY NOTES

Approved for public release; IAW AFR 190-17

JOSEPH P. HIPPS, Major, USAF
Director of Information 1-23-79

19. KEY WORDS (Continue on reverse side if necessary and identify by block number)

III-V Compounds, Gallium Arsinide, Electrical Characterization, Anodic Oxides, Isothermal Dielectric Relaxation Current

20. ABSTRACT (Continue on reverse side if necessary and identify by block number)

The theory and practical limitations of the IDRC technique of Mar and Simmons are discussed. An improved version of the original experiment that incorporates digital processing of the data is described. Results were obtained for Si and used to establish confidence in the new procedure. Anodic oxides of GaAs were then studied, and the results indicate that there are large densities of both fixed and mobile trap states at and near the interface. The mobile trap states behave as though negatively charged.

DD FORM 1 JAN 73 1473 EDITION OF 1 NOV 65 IS OBSOLETE

UNCLASSIFIED
SECURITY CLASSIFICATION OF THIS PAGE (When Data Entered)